CHARACTERIZATION OF ALUMINA TRIHYDRATE ADDED ACRYLONITRILE-BUTADIENE-STYRENE

CHEN SI QI

A project report submitted in partial fulfilment of the requirements for the award of Bachelor of Engineering (Hons.) Chemical Engineering

Lee Kong Chain of Faculty of Engineering and Science
Universiti Tunku Abdul Rahman

April 2015

DECLARATION

I hereby declare that this project report is based on my original work except for citations and quotations which have been duly acknowledged. I also declare that it has not been previously and concurrently submitted for any other degree or award at UTAR or other institutions.

Signature : _____

Name : CHEN SI QI

ID No. : 10UEB04336

Date : 13th April 2015

APPROVAL FOR SUBMISSION

I certify that this project report entitled **"CHARACTERIZATION OF ALUMINA TRIHYDRATE ADDED ACRYLONITRILE-BUTADIENE-STYRENE"** was prepared by **CHEN SI QI** has met the required standard for submission in partial fulfilment of the requirements for the award of Bachelor of Engineering (Hons.) Chemical Engineering at Universiti Tunku Abdul Rahman.

Approved by,

Signature : _____

Supervisor : Dr Bee Soo Tuen

Date : 13th April 2015

Specially dedicated to

my dearest parents, my lovely supervisor and friends

ACKNOWLEDGEMENTS

I would like to express my utmost gratitude to my research supervisor, Dr Bee Soo Tuen for her invaluable advice, guidance and enormous patience throughout the development of the research. She continually conveyed a spirit of adventure in regard to the researches and possessed genuine enthusiasm in regard to teaching. Without her guidance and persistent help this dissertation would not have been possible.

Besides that, I would like to express my deepest appreciation to my project advisor, Ir Dr Lee Tin Sin for his assistance and guidance throughout the project. I would also like to express my sincere appreciation to Mr Ng Hon Meng, Mr Ang Rui Ren, and Mr Lim Kien Sin for their enormous patience in guiding me for the laboratory equipment operation.

In addition, I would also like to express my gratitude to the personnel in University Tunku Abdul Rahman and Nuclear Agency Malaysia who have offered the resources and assistance that are very much required for the completion of this research.

CHARACTERIZATION OF ALUMINA TRIHYDRATE ADDED ACRYLONITRILE-BUTADIENE-STYRENE

ABSTRACT

In this study, the effect of ATH particles and electron beam irradiation on the mechanical characteristics and the flame retardancy of acrylonitrile-butadiene-styrene (ABS) were carried out. Characterisation was made according to the mechanical properties, flammability, surface morphologies and gel fraction of the ATH added ABS composites. The results of tensile test showed that the mechanical properties of the non-irradiated composites deteriorated with the presence of ATH particles. This was due to the poor interfacial adhesion between the ATH particles and ABS matrix. The gel content analysis has suggested that agglomeration have occurred in the composites. The formation of agglomerates could be attributed by the poor dispersion of ATH during the process of extrusion moulding. Scanning electron microscopy (SEM) images have confirmed the presence of agglomerate and the compatibility of ATH particles with ABS matrix was observed to be poor. The application of low irradiation dosage (50-100 kGy) on the samples gradually improved the mechanical properties. However as further irradiation dosage was applied (150-250 kGy), the mechanical properties deteriorated. The gel content analysis suggested that at low irradiation dosage the crosslinking was dominant where at high irradiation dosage chain scission was dominant. The limiting oxygen index (LOI) showed that the flame retardancy of the composites improve significantly with increasing loading level of ATH. The thermal decomposition of ATH would lead to the formation of alumina (char) and water vapour that could inhibit the combustion process. Furthermore, increasing irradiation dosage also improved the LOI values as the crosslinking network formed in the polymer matrix was more stable to resist the formation of volatiles polymer.

TABLE OF CONTENTS

LIST OF TABLES

LIST OF FIGURES

LIST OF SYMBOLS / ABBREVIATIONS

c	specific heat capacity, J/kg·K
D	received dose, kGy
eV	electron volt, J
G	g-value
G(S)	g-value for chain scission, eV^{-1}
G(X)	g-value for crosslinking, eV^{-1}
H	heat of enthalpy, kcal/mole
Mn	average molecular number of exposed polymer, mol
Mn,o	initial average molecular number, mol
NA	avogrado's constant, mol^{-}
q	heat energy, J
SE	specific energy, kJ/mole
T_g	glass transition temperature, ^oC
vol.%	volume percent, %
W_1	weight after extraction, g
W_2	initial weight, g
wt.%	weight percent, %
εmax	elongation at break, %
σR	ultimate strength, MPa
σy	yielding stress, MPa
ABS	acrylonitrile-butadiene-styrene
AN	acrylonitrile
ASTM	american society for testing and materials
ATH	aluminium trihydride
CPP	powdered polypropylene-co-ethylene
EPDM	ethylene-propylene-diene elastomers

EVA	ethylene-vinyl acetate
HB	horizontal burning
LDPE	low density polyethylene
LOI	limiting oxygen index
MFI	melt flow index
MH	magnesium hydroxide
PB	polybutadiene
PE	polyethylene
phr	parts per hundred parts of resin
PTFE	polytetrafluoroethylene
PVC	polyvinyl chloride
rpm	revolutions per minute
SAN	styrene-acrylonitrile
SEM	scanning electron microscope
TEM	transmittance electron microscopy
TGA	thermal gravimetric analysis
UV	ultraviolet
XRD	x-ray diffraction

CHAPTER 1

INTRODUCTION

1.1 Background

Acrylonitrile-butadiene-styrene (ABS) is a synthetic engineering resin commonly made up of 70 parts of (70:30 styrene-acrylonitrile copolymer) and 40 parts (63:35 butadiene-acrylonitrile rubber) (Brydson, 1999). It is one of the most important polymers due to excellent properties such as high impact resistance, good stiffness, high dimensional stability at elevated temperature and excellent surface quality (Ebewele, 2000). The ABS has high processability along with good surface glossiness. ABS has achieved wide applications in machinery, vehicles and electric products nowadays. In recent years, there is increased demand of ABS polymers in the automotive sector in order to achieve weight reduction by the replacement of metals with ABS due to its toughness and strength. Acrylonitrile imparts chemical resistance and high strength, and butadiene provides ductility and impact strength where styrene contributes rigidity and ease of processing characteristics. Different

A major drawback of ABS polymer is its poor flame resistance. ABS is rated as HB (horizontal burning), the lowest rating for UL-94 flammability test. HB is a slow burning rating where it takes more than 3 minutes to burn four inches of the object. During combustion ABS will release hydrocarbon gas which acts as fuel and self-perpetuates until the fuel source has ran out. As ABS burns slowly there is high risk of the occurrence of dripping which will exacerbate the combustions. Therefore it is necessary to construct a flame-retarded composition for ABS to minimize the spreading and continuous combustions.

Alumina trihydrate (ATH) is the most widely used flame retardant and smoke suppressant due to its versatility, low cost and non-carcinogenic. The flame retardants that were traditionally used such as bromine and chlorine are found to be harmful to living beings (Dunnick and Nyska, 2009). It can be used in a wide range of polymers at processing temperatures at and below 200°C (Wilkie and Morgan, 2009). During combustion ATH decomposes to form alumina (Al_2O_3) releasing water molecules. The reaction is endothermic and ATH absorbs up to 1.3 kJ g^{-1} of the energy to form water vapour. The water vapour will dilute the radicals in the flame reducing the surrounding temperature while the residue alumina builds up char, a form of barrier preventing oxygen reaching the fuel. The fuel starvation will stop the combustion (Hull, Witkowski and Hollingbery, 2011).

Hydroxides flame retardants however is relatively ineffective compared to halogen additives and requires addition amount of hydroxides up to 60 % by weight to achieve effective fire resistance (Le Bras, et al., 2005). Camino et al (2001) have successfully achieved useful flame retardancy level of ethylene-vinyl acetate copolymer with overall magnesium hydroxides/ ATH filler loading higher than 50 wt.%. Hornsby and Watson (1989) have conducted studies on the addition of magnesium hydroxide into ABS by 50 % 60 % weight of the filler and discovered there are improvements on the properties on ABS. The above studies provide valuable information for this study as the effects of ATH on ABS have not been extensively studied.

High loadings of ATH, however, will cause dilution of polymer and thus deteriorate the mechanical properties of the polymer (Le Bras, et al., 2005). The ATH added ABS composite has to be treated in order to retain its mechanical properties while imparts acceptable flame retardancy. Irradiation techniques have been employed to induce crosslinking of polymers to improve the mechanical properties of the polymer. Commonly, electron beam and gamma irradiation were employed to induce crosslinking in polymers. The irradiation of polymers can generate high-energy free radicals that form C–C intermolecular bonds between the long molecular chains (cross-linking) to enhance inter-chain interaction (Ng, et al., 2014). These radicals produced will initiate reactions such as cross-linking and chain

scission where cross-linking increase molecular weights and chain scission reduces the molecular weight (Narkis, et al., 1985).

Cross-linking will connect different polymer chains into a bigger network increasing the molecular weight of the polymer (Brydson, 1999). Cross-linking causes the increases of the composites molecular weight (Narkis, et al., 1985) where a change in molecular weight will induce change in viscosity/free volume which in turn affect the polymer microstructure (Torikai, Murata & Fueki 1984). The degree of crosslinking depends upon the polymer and radiation dose. An advantage of using irradiation for crosslinking is that the amount of crosslinking is controlled by the amount of dose of radiation. In Ramani and Ranganathaiah (2000) study, cross-linking is dominant in ABS after irradiated with ultraviolet (UV) ray. The difference of UV ray and electron beam is that the former projects lower energy than the latter onto the polymer which suggested it was possible that cross-linking will dominate in ATH added ABS composites that undergo electron beam radiation.

1.2 Problem Statements

Acrylonitrile-butadiene-styrene has low flame retardancy which can be improved by adding ATH in order to achieve publicly acceptable flame retardancy. Due to the ineffectiveness of ATH, high loadings of alumina trihydrate were required in order to achieve acceptable flame retardancy level. High loadings of ATH reduced the concentration of ABS polymers which would deteriorate the properties of ABS. Therefore, ATH added ABS needs to be treated with radiation to improve its properties. The problem statements are stated as follow:

I. What is the effect of increasing loading level of alumina trihydrate on the flame retardancy, mechanical, physical and thermal properties of ABS?
II. What is the effect of increasing the electron beam irradiation dosages on the flame retardancy, mechanical, physical and thermal properties of alumina trihydrate added ABS composites?

1.3 Aims and Objectives

The main objective of this study was to investigate the effect of increasing electron beam irradiation dose on the flammability and mechanical properties of ABS polymers filled with various ATH loading levels before and after thermal aging. The main objectives were stated as follow:

I. To determine the optimal amount of alumina trihydrate required to achieve the required flame retardancy while maintaining mechanical, physical and thermal properties of ABS.
II. To investigate the electron beam dosage that can improve the mechanical, physical and thermal properties of the alumina trihydrate added ABS composite comparable to that of pure ABS polymer.

1.4 Scopes

To meet the objectives of the study the sample, the following scopes were identified:

I. Preparation of ATH and ABS composites

   a. The alumina trihydrate and acrylonitrile-butadiene-styrene were compounded using a twin screw extruder at temperature of 180 ^{o}C. The compounded ATH added ABS composites were compression moulded into 1-mm polymer sheet using the hot press machine. The 1-mm thickness sheet was then being electron beam irradiated using an electron beam accelerator.

II. Characterization Test

   a. Tensile Test

      The tensile test would be performed using Instron Tensile tester in accordance to ASTM D1822. This test was used to measure the tensile strength and elongation at break of the ATH added ABS composites.

b. Gel Content Test

The gel content test was carried out in accordance to ASTM D2765. This test was used to measure the degree of crosslinking of the ATH added ABS composites.

c. Limiting Oxygen Index Test

The limiting oxygen index (LOI) test was conducted according to ASTM D2863. This test was conducted to determine the LOI value, flammability indication, of the ATH added ABS composites.

d. Scanning Electron Beam Microscopy Test

Scanning electron beam microscopy (SEM) test was used to examine the morphology and microstructure of the ATH added ABS composites. The equipment that would be used for this test is JEOL model JSM-6301F field emission scanning electron microscope.

CHAPTER 2

LITERATURE REVIEW

2.1 Combustion of Polymers

Polymers are made up mostly of hydrocarbons which make them highly combustible (Pal and Macskasy, 1991), as the decomposition products are often highly flammable. Combustion reaction requires three factors: Heat, fuel and oxygen. Combustion reactions can be generally separated into several stages as follow:

1. To initiate a combustion reaction, an external heat source must be applied to the polymeric material. The temperature of the polymer materials will increase according to the rate of heat supply and the thermal and geometrical characteristics of the polymer.
2. With continuous supply of heat source, the polymer chains experience decomposition. The volatile radicals of the resulting polymer fragments will diffuse into the surrounding where they combined with the oxygen in the atmosphere producing combustible gaseous mixture.
3. This gaseous mixture will ignite as the auto-ignition temperature is reached or alternatively, the fuel may ignite at flash point if external energy is supplied. The ignition releases large amounts of heat which is then absorbed by the underlying polymer causing further polymer bonds scission. (Brydson, 1999)
4. Combustion is followed by the ignition when the amount of heat released reaches a significant level and increased the intensity of combustion (Hornsby, 2001).

5. New thermal decomposition will be induced as the amount of heat released reaches a sufficient level which is known as the propagation of combustion. The duration of the combustion reaction relies on the amount of heat released during the combustion of the fuel (Laoutid, 2008).

6. Large amounts of smoke and toxic gases may evolve during combustions which are notably known to have caused higher casualty than burning does (US Fire Administration, 2013).

2.2 Acrylonitrile-Butadiene-Styrene (ABS)

2.2.1 Chemical Structure and Thermophysical Properties of Acrylonitrile-Butadiene-Styrene (ABS)

Acrylonitrile-butadiene-styrene (ABS) contains three monomeric units, acrylonitrile, butadiene and styrene as shown in Figure 2.1. Acrylonitrile is a colourless liquid with a strong odor. At atmospheric pressure, it has a boiling point of 77.3 ^{o}C and a melting point at -83 ^{o}C. Acrylonitrile is soluble in both polar and non-polar solvent where the water solubility will increase with temperature (Code of Federal Regulations 2012). The homopolymerization of acrylonitrile monomer occurs at the carbon-carbon double bond with the present of free radicals as initiators. The product, polyarylonitrile, however is insoluble in most solvent, a reverse opposite property of that to an acrylonitrile monomer. 1,3-Butadiene has a boiling point of -4.414 ^{o}C and a melting point at -113 ^{o}C, which make it a gas in room temperature (25 ^{o}C) (Herman, 2007). Butadiene is a very reactive compound due to the presence of two carbon double bonds. Polybutadiene (PB) is formed by addition polymerization (Saltman, 1965). Styrene is a slightly yellowish and oily liquid. The boiling point of styrene is around 145 ^{o}C (Whelan, 1994) and the boiling point is -30.6 ^{o}C. Styrene homopolymerization can occur by ionic reactions or free radical reactions (Platt, 1970).

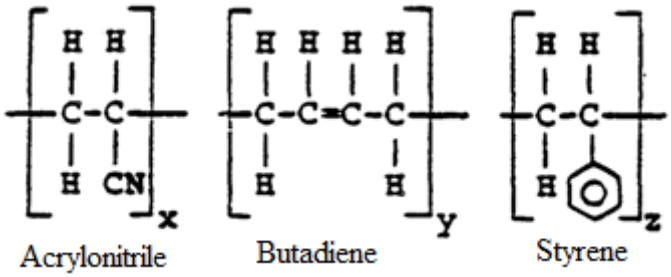

Figure 2.1: Chemical Structure of Acrylonitrile-Butadiene-Styrene (Bohen and Lovenguth, 1989).

2.2.2 Preparation of Acrylonitrile-Butadiene-Styrene

Acrylonitrile-Butadiene-Styrene can be manufactured by two general methods: Emulsion polymerization and mass polymerization. For emulsion polymerization there are three processes: batch, semi-batch and continuous. The first step for emulsion polymerization is to prepare PB latex with batch process for each of the process. 1,4-butadiene polymerization will produce cis and trans double bond in the PB backbone while 1,2-butadiene polymerization will produce pendant vinyl groups. The resultant polymers depend on the temperature of the polymerization instead of the concentration of butadiene. Crosslink density and PB particle size is controlled by the addition of chain transfer agents and various additives. Agglomeration of PB particle is usually performed to increase the particle size. The degrees of crosslinking and particle size depend on the end-product specification. Next, styrene and acrylonitrile will be polymerized in the presence of PB seed particle which will then result in the grafting of SAN onto PB during the polymerization. While for mass polymerization, the PB used is un-crosslinked and it is dissolved in a mixture of acrylonitrile and styrene monomers. Initiators have to be applied to start the polymerization in a pre-polymerization reactor (Colborn, Buckley and Adams, 1993).

2.2.3 Processing of Acrylonitrile-Butadiene-Styrene

Additives, flame retardant fillers or other chemical reagents are compounded with ABS in order to achieve the desired ABS grades. Compounding is done by using extruders. The desired melting temperature of ABS is 221-240 ^{o}C while flame retardant ABS grade is not as thermally stable thus the melting temperature should not exceed 246 ^{o}C. The temperature suggested by literature is shown in Table 2.2. In extrusion, the molten polymer is added with the respective additives which are then forced forward by the turning screw(s) and are pushed under pressure through a die. Wearing occurs from the rubbing of the molten composites on the die surfaces. The die diameter used is commonly about 1/8 inch. The filled plastic emerges as spaghetti-like strands which are then cooled with water or air followed by the cutting of the composite strands into cylindrical pellets about 1/8 to 1/4 inch long (Ciullo, 1996).

Table 2.1: ABS Extrusion Temperature Guidelines (Giles, Wagner and Mount, 2005)

Zone	Conditions	Temperature Setting , ^{o}C
1	**Melting: heating and melting to achieve partial or total mixing**	177-193
2	**Venting: removing volatiles and moistures**	199-216
3	**Mixing: ensure proper mixing**	210-227
4	**Vacuum: Completely remove volatiles and moistures to required level**	216-240
5	**Metering: Building up the required pressure at the die**	216-240
6	**Adapter**	226-240
7	**Die**	210-240

2.2.4 Physical, Mechanical and Thermal Properties for Typical ABS

Acrylonitrile-butadiene-styrene consists of two distinctive phases with differing properties where SAN is hard, transparent and relatively brittle thermoplastic, while crosslinked PB is soft and elastomeric. The PB is grafted with a copolymer of styrene

and acrylonitrile (SAN) and embedded in a SAN matrix. The SAN copolymer that is chemical bonded to PB is referred to as grafted SAN while the fragment of SAN copolymer that is not bounded is referred to as free-SAN. The physical properties of ABS are intermediate between glass and rubber, while the mechanical properties, prone to be similar to glassy material than rubber with the exception of its impact toughness (Colborn, Buckley and Adams, 1993). Acrylonitrile-co-styrene imparts chemical resistance, process ability and rigidity, and butadiene provides ductility and increase impact resistance. Generally, the strength and rigidity of ABS increases as the SAN content increases whereas as the PB content increases the strength and rigidity of the ABS reduces (Whelan, 1994). The ABS is naturally opaque with a yellow tint when the dispersed phase is based on emulsion particles and opaque to translucent white for those of bulk particle. ABS chemical resistant is strong for acidic and basic solution but is susceptible to polar solvent attack. The details of the two phases and interfacial region are the most significant factor affecting the mechanical properties of the resulting ABS compound.

Table 2.2: **Properties of ABS with Respective Maximum and Minimum Values (Giles, Wagner and Mount, 2005)**

Property	Maximum	Minimum
Specific Gravity	1.07	0.99
Tensile Strength, psi	11,000	2500
Flexuran Modulus, psi	500,000	100,000
Izod, ftlbs/in	13.0	0.8

The morphology of the modifying phase will strongly affect the ABS properties. The morphological parameter that is important for rheology study is the gel-fraction. Gel-fraction is the volume fraction of the dispersed phase and the grafted SAN. This volume fraction controls almost all of the mechanical properties of ABS

The mechanical properties of ABS can be divided into two groups according to strain rate:

i. Those that relate the low strain rate behaviour, such as the elastic, creep and isothermal fatigue behaviour;

ii. Those obtained under high strain rate of impact conditions.

The elasticity of a two distinctive phases is affected by the volume fractions of the two phases. The elasticity of ABS can be modified by the PB volume fraction in proportion to the SAN matrix. The rubber phase has very low modulus, approximately 1MPa, while SAN modulus is 3000 MPa. Thus the addition of the second phase reduces the elastic modulus proportional to the volume fraction occupied by that phase. Typical elastic modulus values for SAN are between 3000 and 3600 MPa. Elastic modulus of ABS is dependant of the polybutadiene loading but it is approximated at 2000 MPa. The load-displacement curve for a typical ABS in a tensile test shows a quasi-elastic region extending up to 0.50 to 0.75% strain, followed by a yielding at stresses in the order of 4 to 6 MPa, and a strain softening region in which the load roughly remains constant until failure. The elongation at break is about 30% and increases with increasing the rubber content. Higher strain rates reduce elongation but increase the yield strengths and elastic modulus.

The impact toughness of ABS is a function of all its material parameters, with greatest dependence on the rubber phase: volume fraction, graft or interfacial morphology, and degree of crosslinking. To interface must be able to transfer stress from the matrix to the rubber particles in order to achieve higher impact properties. Particles that are not well bonded to the matrix will act as voids, resulting in reduced toughness. (Gao, Wang and Kim, 2005). The impact toughness of ABS is insensitive to the radius of the notch used, sub-millimetre notch radii produces no significant loss in toughness. Notched impact values range from 105 to 440 J/m. The addition of rubber improves the strength of the SAN when impacted at high strain rates. Without the rubber phase, SAN is a brittle glassy polymer with very low elongation to break and gives a notched Izod impact strength of about 25 J/m. The rubber particles enable the matrix to yield under plastic deformation by several energy-absorbing mechanisms:

i. shear yielding

ii. crazing

iii.cavitation

Shear Yielding is applied to test the ductility of a material where crazing is often precedes fracture in glassy thermoplastic polymer which is semi brittle. Cavitation is formed during the deformation of brittle polymers. Deformation consists of extensive

shear deformation assisted by multiple crazing originating at the rubber particles and cavitation within the particles. Cavitation is responsible for the dilational strain in ABS. The changing of the material composition affects the balance between shear and cavitation. Rubber particle cavitation will create plane stress conditions within the closely packed particles in the matrix material and allows ligaments to deform by yielding instead of cracking. Increasing the strain rate will prone to forming crazing and cavitation, from shear yielding at a lower strain rate. The SAN matrix ratio has several effects on mechanical behaviour: Higher acrylonitrile content results in higher ductility deformation which is due to having higher strand density in the matrix. When this happens, the balance of deformation tends to shift away from crazing and forms shear. Shear is more preferred among the two mechanisms because no voids are created in the process as it is in craze. High temperature, low strain rates and orientation all shift the deformation mode towards shear (Colborn, Buckley and Adams, 1993).

The flammability of ABS can be denoted by the heat release, flame-spread rate and ignitability. The most common used laboratory test method is the limited oxygen index (LOI). The LOI value represents the amount of minimum oxygen concentration that can sustain the combustion for 3 min or combust the sample of 5cm length placing the sample in a vertical manner. The LOI is obtained from the following formula:

$$LOI = 100 \text{ x } \frac{Oxygen}{Oxygen+Nitrogen\,(Air)} \qquad \text{(E 2.1)}$$

where

LOI = limiting oxygen index, %

Materials with LOI below 21 is considered to be combustible because once ignited the atmospheric oxygen is sufficient to sustain the fire. Materials with LOI above 21 are considered to be self-extinguishable because the oxygen in the atmosphere is not sufficient to sustain the fire without supplying external energy sources. Therefore, the higher the LOI, the flammability property is better. The LOI value for a typical ABS is 19 % which is lower than the atmospheric oxygen concentration of 21 % (Mouritz and Gibson, 2007).

2.2.5 Thermal Degradation of ABS at Elevated Temperatures

The uses of ABS in the automotive industry require it to be durable in extreme environmental weathering and heat aging. Thermoplastic, like ABS when heated will soften and melt before decomposing. For ABS, degradation starts with the abstraction of hydrogen by oxygen. The reaction is thermodynamically preferable because of the presence of tertiary substituted carbon atoms in the PB phase. Sufficient thermal energy will activate the hydrogen abstraction to initiate oxidation, speeding the rate of degradation. The mechanical properties of ABS such as elongation at break and impact strength would deteriorate causing premature failure (Wolkowicz and Gaggar, 1981 cited in Tiganis, et al., 2002, p.425). Shimada and Kbuki (1968) proposed that thermo-oxidative degradation is confined in the rubber phase forming hydroperoxides. The degradation caused by hydrogen abstraction is suggested to happen in the PB phase. In contrast, Wyzgoski (1976) discovered that the degradation of ABS is due to a combination oxidation in the PB phase and physical aging in the SAN phase. The author has also found the elongation loss by thermal aging of ABS subjected to the temperature below the glass transition temperature is recoverable by reprocessing.

The degradation in SAN phase depends on the difference in the aging temperature and the glass transition temperature (T_g) of SAN, which is at 113 ^oC (Wyzgoski, 1976). If the aging temperature is below the T_g physical aging tends to occur, whereas thermo-oxidative degradation will occur if aging temperature is higher than T_g (Clough, Billingham and Gillen, 1996). According to Tiganis, et al., (2002) the impact resistance of SAN decreases from 27 kJ/m^2 to 14 kJ/m^2 aging at 105 ^oC for 672 hours. Even though the gaining temperature is lower than T_g but the discolouration in specimen showed that thermo-oxidative degradation of ABS specimens is also possible. The author has showed evidence that physical aging would induce slight increase in Young's modulus in the ABS specimen aged at 90 ^oC.

The degradation in PB phase is induced by production of hydrogen free radicals from the carbon atom. The free radicals in turn form carbonyl and hydroxyl. Referring to the reaction mechanism by Shimada and Kabuki (1968) further degradation might facilitate formation of crosslinking or polymer peroxides

(hydrogen peroxides for example). Thermo-oxidation of PB phase will increase the Young's modulus and making the composite more brittle. Tiganis, et al., (2002) found that there is significant reduction in the absorbance band of FTIR spectra, indicating changes in the PB microstructure. The changes might be induced by crosslinking or chain scission. Crosslinking of the polymer chains will reduce mobility and free volume in the PB phase which can be detected using PALS. The author has found that at aging 120 ^{o}C, which will reduce the relative free volume fraction, while increasing the Young's Modulus and reduced the tensile strength of the specimens up to 30 %. Whilst the properties are relatively constant for aging at 90 ^{o}C. The degradation in the PB phase has more significant effect on the deterioration of the ABS mechanical properties than degradation.

2.3 Flame Retardants

Flame retardant is the compound incorporated into polymers to reduce the impact of fires on the safety of people, environment and property. Flame Retardant are substances that can be chemically bonded into the polymer molecule or be physically blended in polymers after polymerization to inhibit, suppress, delay or modify the propagation of a fire through a polymer material. Flame retardant interfere a specific stage during combustion. There are several classes of flame retardants; Halogenated Hydrocarbons, Inorganic flame retardants, Phosphorous containing compounds (Frca, 1998). Flame retardants can be classified in two categories:

Table 2.3: Flame Retardants and Respective Method of Processing (Laoutid, 2008)

Category	Method of Processing
Additive flame retardants	incorporated during the transformation process and do not react at this stage with the polymer but only at higher temperature.
Reactive flame retardants	incorporated during synthesis process (as monomers or precursor polymers) or post-reaction processes (e.g. via chemical grafting). Such flame retardants are integrated in the polymer chains

To be an effective flame retardant, its decomposition temperature must be approximately near to that of the polymer it is incorporated. Flame retardants can react chemically and or physically in solid, liquid and gas phase. They do not interfere only in a single stages, there are several reactions happening simultaneously with one dominating (Bourbigot and Duquesne, 2007). There are various modes of thermal degradation effect from various flame retardants.

Two of the most significant chemical reactions on interfering combustion occur in the gas phase and condensed phase (Le Bras, et al., 2001;Bourbigot and Duquesne, 2007). There are two possible reactions triggered in condensed phase: (Bourbigot and Duquesne 2007;Laoutid, 2008)

i. Accelerate the decomposition of the polymer thus increases the flow of polymers drips. The drips will withdraw away from the flame source hence, quenching the fire;
ii. The formation of carbonized layers (char), ceramic-like, or glass on the polymer surface by the degraded polymers

The formation of char has significant effect on the fire retardancy. Char is formed as a decomposition product of the polymer composite that is comprised of only carbon, removing hydrogen and oxygen from the polymer.

The gas phase can be understood as the radical mechanism of the combustion taking place in gas phase is interrupted by the flame retardant or respective degraded products. The early flame retardant is halogen based operates in gas phase with inhibiting effect. It is favoured due to the high flame retardancy with low loading. The halogens, Cl^- or Br^-, form halogen halide, a more stable species, with the free radicals, H^+ and $OH\cdot$ which are responsible for the propagation of fire, thus inhibiting the propagation of fire (Hull, Witkowski and Hollingbery, 2011). The by-products by incomplete combustion are highly toxic, for instance hydrogen chloride produced has higher toxicity than carbon monoxide. Halogen based flame retardant is also of environmental concern because of their high lipophilicity and high resistance to degradation processes. The resistance to be metabolised will result in bioaccumulation and encourage malignancy (Rahman, et al., 2001). Furthermore, the is potential of extremely toxic dioxin exposure to the environment by halogenated diphenyl ether, such as polychlorinated biphenyls which have raised great concerns,

not only in the scientific community but from the government and public on the safety of halogen based flame retardant (Zaikov and Lomakin, 2002) including the widespread distribution of flame retardant detected in remote areas such as the Artic and deep oceans subsequently induced large number of researches on halogen-free flame retardant. The introduction of flame retardants changes the morphological structure of a two phase material. The flame retardant distribution in the polymer will affect the performance of the filled polymer. Point A, B and C are three points where flame retardant interrupts the fire cycle. To increase the effectiveness of a flame retardant, it should be able to break the cycle in two and more break the cycle of combustion in more than two points.

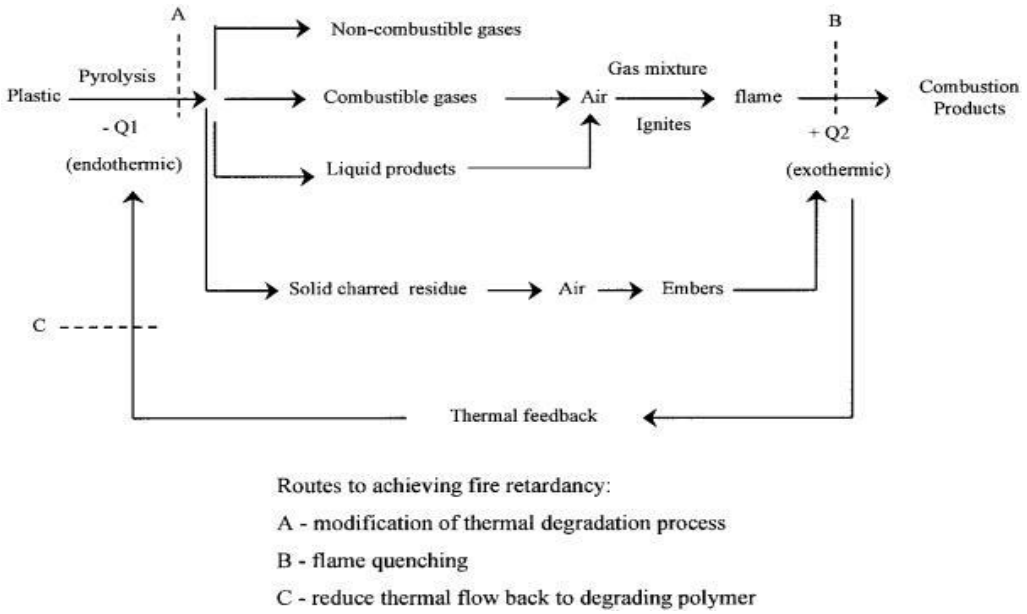

Figure 2.2: The Stages in Polymer Combustion (Hornsby, 2001)

2.3.1 Flame Retardant Mineral Fillers

The ideal characteristics required from that of effective flame retardant fillers are:

1. Highly endothermic decomposition in the temperature range of 100-300 ^{o}C releasing at least 25 % by weight of water and/or carbon dioxide.
2. It is readily available and low in cost
3. Low toxicity and low toxicity in thermal decomposition products

4. Can be obtained in small particle size and sufficiently low surface area which is able to be used at high loadings
5. Low levels of detrimental impurities
6. Colourless

Presence of fillers in polymer strongly affects polymers combustion characteristics. Incorporation of mineral fillers will reduce the flammability of polymer by increasing the heat capacity, heat conductivity and/or reduces the content of combustible products. The fillers will also modify the polymer thermophysical properties and changes the viscosity of the decomposition products. However, fillers cannot be said to be totally inert in terms of their effect on the behaviour of polymer combustion. The most commonly used mineral flame retardants are metal hydroxides, hydroxycarbonates and zinc borates. These inorganic fillers have a direct physical flame retardant action (Hull, Witkowski and Hollingbery, 2011). Apart from the mentioned flame retardant effects, hydroxides and carbonates can be expressed as follow:

i. **By Dilution:** Inert fillers and additives that evolve inert gases upon combustion dilute the fuel formed in pyrolysis, hence quenching the fire; (Horrocks and Price, 2001).
ii. **By Cooling:** The additives degrade endothermally reducing the polymer temperature below that is required to sustain the combustion process; (Bourbigot, et al., 1999).
iii. **By formation of a protective layer:** External flame retardant coating is applied to prevent the interactions between oxygen and the polymer surface. This will reduce the heat transfer from the fire to the polymer which will then reduce the supply of fuel for propagation of fire (Horrocks and Price, 2001).

Smoke suppression is observed in ethylene-propylene-diene(EPDM) elastomers (Moseman and Ingham, 1978) proplylene (Hornsby and Watson, 1989) and ABS (Hornsby and Watson, 1990) that are incorporated with hydrated fillers. Fillers can reduce the overall level smoke released as well as to delay the smoke evolution.

2.3.2 Factors Affecting the Mode of Actions of Hydrated Flame Retardant Fillers

There are three primary modes of actions as mentioned above: gas phase, condensed phase and physical/chemical effects. In each form, there are several factors that influence the performance of the fillers. The factors affecting the mode of actions are tabulated in Table 2.4.

Table 2.4: Factors Affecting Respective Mode of Actions of Hydrated Flame Retardant Fillers (Hornsby, 2001).

Gas Phase	Condensed Phase	Physical/Chemical
Water/gas evolution	Thermal Effect from filler endotherm	Particle size/Surface area
Cooling Effect	Heat Capacity	Particle Morphology
Dilution of combustion products	Thermal Feedback	
	Dilution of combustible polymer	
	Filler-polymer interaction	
	Relative decomposition temperature of filler and polymer	
	Char/residue formation	

2.3.3 Mode of Actions of Metal Hydroxide in Polymers

Metal hydroxides first mode of action is through gas phase action by releasing water vapour through endothermic decomposition at a temperature higher than the polymer processing temperature range, and around the polymer decomposition temperature. Second mode of action is through condensed phase that the thermally stable inorganic residue will build up to form a protective layer (Hull, Witkowski & Hollingbery 2011). Metal hydroxide does not have water in the molecule structure but the hydroxyl group will produce water when decomposed endothermally. The charring layer is very unreactive thus acting like a barrier between the fire and the

polymer. Researches have shown that substantial amount of metal hydroxides are required for effective flame retardancy.

Table 2.5: Combustion Reactions and Thermal Degradation Mechanism (Le Bras, et a., 1998)

Mode of Action	Combustion Reaction	Mechanism
Endothermic Reaction	$H\cdot + O_2 \rightarrow OH\cdot + O\cdot$ $O\cdot + H_2 \rightarrow OH\cdot + H\cdot$ $OH\cdot + CO \rightarrow CO_2 + H\cdot$	X-OH + heat → Char + H_2O

2.4 Alumina Trihydrate

2.4.1 Preparation of Alumina Trihydrate

Alumina trihydrate (also known as aluminium hydroxide) is commercially produced by Bayer process from mineral bauxite. Bauxite contains about 40 to 70 % of alumina trihydrate, principally gibbsite and boehmite. The mineral is dissolved in sodium hydroxide to form sodium aluminate solution, followed by controlled precipitation. It is a low cost production due to the ability for the flame retardant grade alumina to act as an intermediate product for alumina manufacturing of major scale. Ground Bayer hydrate owns the largest volume of ATH sold as flame retardant in particle size ranging from 1.5 to 35 μm. The drawback of this low cost production is the formation of many irregular shaped particles which proves to be unsuited for various applications. The second largest production for ATH is the precipitation of ATH from purified sodium aluminate, applying conditions that is capable of controlling the resultant particle size and shape and eliminate the need for milling. The particle size ranges from 0.25-3 μm (Wilkie and Morgan, 2009). Alumina trihydrate is hydrophilic where most of the polymers are hydrophobic making both materials repelling each other. In order to increase the compatibility of ATH to polymer, ATH is commonly treated with stearic acid (Jia, 2005).

2.4.2 Properties of Alumina Trihydrate

The typical properties of ATH is shown in Table 2.6. In a purified form, it is an odourless white powder or granule. In water, aluminum hydroxide shows amphoteric behaviours in which it will act as acid in the presence of a strong base and as a base in the presence of a strong acid. The reactions are simplified as follow:

In the presence of hydrochloric acid, the reaction forms aluminium chloride.

$$3\ HCl + Al(OH)_3 = AlCl_3 + 3\ H_2O \qquad \text{(R 2.1)}$$

In the presence of sodium hydroxide, the reaction forms sodium tetrahydroxoaluminate.

$$Al(OH)3 + NaOH \rightarrow Na[Al(OH)4] \qquad \text{(R 2.2)}$$

Table 2.6: **Typical Properties of Alumina Trihydrate**

Properties		**Value**
Molecular weight		78.0036 g/mol
Solubility	**Water**	Insoluble
	Solvent	Soluble in strong acids and bases
Density		2.1 - 2.7 g/cm3
Melting Point		300 ^{o}C
Mohs' hardness index		2.5-3.5.

2.4.3 Thermal Decomposition of Alumina Trihydrate

Bonsignore (1981) stated that the endothermic decomposition of ATH occurs around 220 ^{o}C, which is slightly higher than the temperature discovered by Delfosse et al. (1988) and Laoutid (2008), which is 180 to 200 ^{o}C. However there are more studies that showed that the decomposition of ATH initiated from 180 to 200 ^{o}C. The temperature range for decomposition starts from 200 to 400 ^{o}C. Alumina trihydrate decomposition will undergo intermediate reaction producing boehmite starting from 200 to 300 ^{o}C , then at approximate 330 ^{o}C the residue gibbsite decomposed to alumina, indicated in the following figure with the first two peaks (Brown, Clark &

Elliot 1953). Therefore, ATH is only suitable for polymer that has processing temperature below this or around its decomposition temperature. As stated above, the primary mode of action is the decomposition of the hydroxyl groups forming three water molecules, according to the following reaction:

$$2\ Al(OH)_3(s) \rightarrow Al_2O_3(s) + 3\ H_2O(g) \qquad \text{(R 2.3)}$$

This is an endothermic reaction with enthalpy of 1300 kJg^{-1}. Approximate 23 % of gaseous formed (Abdul Aziz, et al., 2012) constituted of the water vapour which will act as a protective gas layer, diluting the percentage of combustible gas mixture surrounding the polymer. The second mode of action of ATH thermal decomposition is the forming of alumina (Al_2O^3) (charring) that will cover the polymer of solid phase isolating the volatile polymer from further heat exchange.

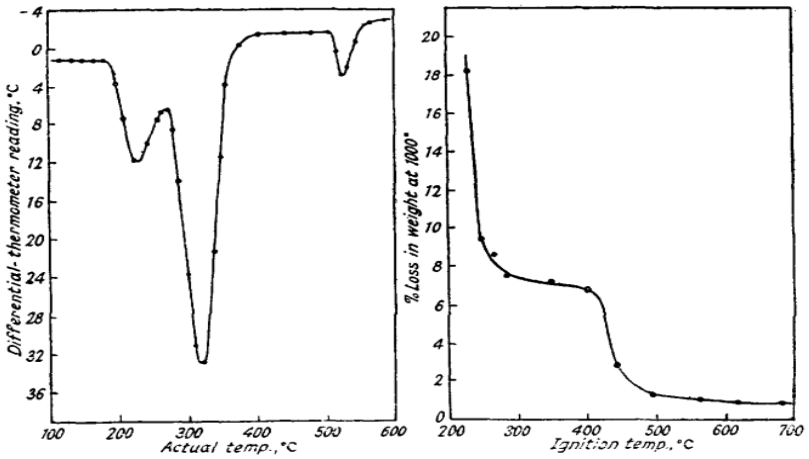

Figure 2.3: The Differential Thermal Analysis Graph and Ignition Temperature Graph (Brown, Clark & Elliot 1953)

Hull, Witkowski and Hollingbery (2011) studied the effect of flame retardant of mineral fillers by quantitative approach. In relative to the flame retardant effects, ATH, the endotherm contributed the most by 55 %, where the water vapour formed contributed 23 % followed by the 13 % of the solid residue and finally the filler contributed only 9 % to the flame retarding effects. The results presented by their work can only provide a qualitative estimation of the actual events as they have adopted several unrealistic assumptions in which that the thermal conductivity of the

polymer composite remained unchanged which is not true. They have assumed that the only effect of the gas phase diluent only absorbs heat neglecting any effects reducing the free radical concentration below a critical threshold.

2.4.4 Effects of Alumina Trihydrate in Polymers

2.4.4.1 Flame retardancy of ATH added Polymer

Aforementioned mode of actions by metal hydroxide in polymer is applied to that of ATH. In summary, ATH decomposes endothermically having an enthalpy of decomposition of 1300 x 10^3 kJ/g. The onset temperature of decomposition is around 180 to 200 ^oC containing 34.5 % by weight of water molecules. Notably the decomposition enthalpy of 1g of ATH is equal to the heat required to increase the temperature of a LDPE of 1.5g from ambient temperature to decomposition which is (400 ^oC). With the assumption of having constant heat capacity throughout the combustion the heat required can be calculated through the following equation:

$$q = mc\Delta T \qquad \text{(E 2.2)}$$

where
q= heat energy, J
m=mass, kg
c= specific heat capacity, J/kg,K
ΔT=change in temperature, K

Delfosse, et al., (1989) discovered that the presence of alumina trihydrate will increase the self-ignition temperature of the EVA specimen composite with increasing fillers concentrations. While heating at temperature lower than the self-ignition temperature the intensity of incandescence formed by the filled EVA is higher than that of pure EVA which is produced along with a significant increase in the sample temperature. This can be interpreted as decreasing the onset temperature for incandescence. The authors also suggested the occurrence of incandescence may

indicate that the filler promotes combustion of the oxidation residue rather than oxidation of gaseous products. The increased self-ignition temperature shows increase of flame retardancy because more heat energy is required in order to decompose the polymer composites.

The addition of ATH is expected to increase the flammability of the polymer in use. Camino, et al., (2001) has recorded that the addition of ATH into the EVA specimen increased the rank of UL94 test from HB to V-2 while the LOI value increased from 9 vol% to about 28-29 vol%. The specimens prepared by the authors containing 50 wt% of ATH. One point worth noting is that the size and surface contact are one of the factors influencing the thermal properties, the larger ATH particle size with smaller surface contact area produces a better combustion test value. The authors conducted the combustion test with mass loss calorimeter. It is found that the minimum ignition time has increased rather significantly from 78 s (pure EVA) to 92 s (ATH with 1.3 μm mean size, 4^2/g-filled EVA). In another specimen of EVA filled with ATH of smaller particle size and higher surface contact area, the time required to ignite has negligible difference with that of pure EVA. Although the time required to reaching the maximum gas temperature is much higher than the pure EVA specimen.

Zhang, et al., (2005) produced a rather similar result with Camino, et al., (2001). The former found that the amount of ATH required to produce effective flame retardancy is 60 wt%, at an interval of 20 % from 0, which passed the UL94 test with V-2 and obtained 30.6 % for LOI. Lower weight percent of ATH did not pass the UL94 test even at 40 wt%. The EVA used constituted of 14 % of vinyl acetate with MFI of 0.4 while the latter applied EVA constitutes of 19 % vinyl acetate with MFI of 0.65. There is negligible difference in the specimen used. From both of the works, it can be summarized that at least 50 % of ATH loadings are required to produce satisfactory flame retardancy with improvements as the loading of ATH increases.

Due to the fact that high loading of ATH is required for effective flame retardancy, many researches are done to reduce the loadings of ATH. Alumina trihydrate remains to be popular despite the high loadings requirement due to its cost

competitiveness. The common approach the researchers are taking is to add other flame retardants or treat the ATH. Merely adding known flame retardants that have better performance than ATH in order to achieve better flame retardancy is not suffice. It is the desired to produce a synergistic effect from the addition of other flame retardants and ATH.

Many researches have been carried out to improve the performance of the ATH, for instance to investigate the effect of lignin with ATH (De Chirico, et al., 2003), nano-CG-ATH (Cui, Guo and Chen 2007) and organoclay added with ATH (Cheng, et al., 2011). In De Chirico, et al., (2003) studies, the addition of lignin improves the polymer flammability as well as for Cui, Guo & Chen (2007) research; the nano-CG-ATH proves to have synergistic effect on the polymer flammability. As for Cheng, et al., (2011) studies, the weight percent of ATH required to pass the UL94 flammability test is 27 % with 3 % of cloisite, which is very much lower than that required of one flame retardant. Three of the studies stated above have one thing in common which is low loadings of ATH and other additives. However it is noted that the polymer tested upon by the flame retardants are different types. Despite the difference in the polymers, the loading of ATH is significant reduced.

2.4.4.2 Smoke Suppression

Smoke is comprised from carbon-rich particles which issue from polycyclic aromatic hydrocarbons (Pasternak, Zinn and Browner, 1982). Initially, nuclei formed which is then slowly agglomerate giving out smoke. Carbon monoxide, the contributor of grey smoke, is a product of incomplete combustion. Thus the factors contributing to smoke formation may be due to incomplete combustion of polymer. The smoke suppression can be due to the complete combustion of the decomposition products leading to the decrease of CO or leading to the hindrance of agglomeration. The decomposition of ATH gives oxides which are active products. During combustion, ATH forms lewis acid sites which can change aromatic molecules into adsorbed positive radicals. This will reduce the formation of aromatic smoke precursors (Delfosse, et al., 1989). However the mechanism of smoke suppression is not clearly

defined, the suppression is thought to be a consequence of the deposition of carbon onto the oxide surface during the decomposition of ATH (Hornsby and Watson, 1989). Oxides are known to have high surface areas and catalytically active which will promote the carbon deposition and subsequent oxidation processes. The reductions of combustion rate due to flame retardancy of ATH also contribute to the inhibition of smoke evolution. The formation of water vapour due to the decomposition of ATH, however, is suggested to have limited effects on the smoke evolution. Hornsby and Watson (1989) shows that the smoke yields from polypropylene compounds consist of MH and magnesium oxide does not differ much. This result is supported by the later work of these two authors in 1990, that the carbon monoxide emission from ABS burning does not show distinctive difference.

2.4.4.3 Char Formation

According to the visual inspection of combusted polymer, a black layer of molten forms of solid is produced on the polymer solid phase. The heat from the surrounding will be transferred back to the polymer thus the char layer act as a heat sink. The combustion of charred material, two main reactions will occur:

$$C + \tfrac{1}{2} O_2 \longrightarrow CO \qquad \Delta H = -26.4 \text{ kcal/mole} \qquad \text{(R 2.4)}$$

$$CO + \tfrac{1}{2} O_2 \longrightarrow CO_2 \qquad \Delta H = -67.9 \text{ kcal/mole} \qquad \text{(R 2.5)}$$

The residue, Al_2O_3 from (R 2.3) favours the second reaction which is more exothermic. The high energy burning of char forms the incandescence observed by visual inspection. (Delfosse, et al., 1989).

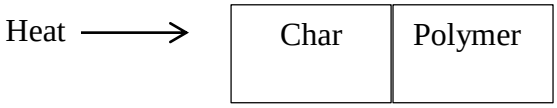

Figure 2.4: Schematic of Heat Transfer

2.4.4.4 Mechanical Properties of ATH added Polymers

To be successful commercially, ATH has to produce acceptable processibility to the polymer formulation in a manner where only minimum reduction of mechanical properties of the composite is required. This is particular difficult for high loadings of ATH. The weight percent of ATH is proportional to the flame retardancy and the deterioration of polymer mechanical properties. High ATH loadings diminish the effect of the original polymers to the overall mechanical performance thus the material will become undesirable. In general, the addition of fillers will increase the elastic modulus accompanied by the reduction in tensile strength and toughness. Furthermore, the interfacial adhesion at the boundary of the filler and polymer matrix has a direct effect on the particulate composite ability to resist crack prorogation (Baillet and Delfossem, 1990). The viscosity of the polymer composite will also increase by the fillers. The addition of ATH will restrain the mobility of polymers by developing small and imperfect crystallites, as the polymer chains cannot move as freely. These defects will induce flaws and submicroscopic cracks (Maurer, et al., 1982). Ethylene vinyl acetate (EVA) has thermoplastic characteristics while being one of the most studied materials incorporated with ATH. From the findings from Camino, et al., (2001), the elongation at break and tensile strength, for the EVA constitutes of 19 % vinyl acetate with MFI of 0.65, decreased significantly with the addition of ATH. The value differences for ATH added EVA is substantial, deteriorating the mechanical properties by more than 50 %. Nabaltec Apyral® 40D and 120D are the ATH added EVA having different ATH median sizes, 1.3 and 0.9 μm respectively. The surface areas of the both composites are 4 and 12 m^2/g respectively.

Table 2.7: Mechanical Properties and LOI of pure EVA and 50 wt.% filler filled EVA (Camino, et al., 2001)

EVA+50 wt % fillers	Tensile test (elongational rate 25 mm/min; T= 20 °C)			
	εmax(%)	**σR(MPa)**	**σy(MPa)**	**LOI (vol %)**
EVA	736±20	30.2±1.5	N/A	9
Apyral® 40D	476±55	12.7±1.5	9.1±0.4	28-28.5
Apyral® 120D	328±69	10.4±0.7	9.8±0.1	28.5-29

As for Zhang, et al., (2005) studies, the tensile strength and elongation at break of EVA reduce with increasing concentration of ATH. The Young modulus increases with the ATH concentration indicates that the addition of ATH will increase the stiffness of the polymer composite. However, the tensile strength and elongation at break are largely reduced making the polymer composite very brittle and easily broken.

Table 2.8: Mechanical Properties and Flammability of EVA Composites (Zhang et al. 2005)

Sample, EVA:ATH (wt%)	LOI (vol %)	UL-94	Young Modulus (MPa)	Tensile Strength (MPa)	Elongation at break (%)
100:0	17.0	Fail	0.80 ± 0.02	15.7 ± 0.1	1635.6 ± 20.6
80:20	18.2	Fail	0.98 ± 0.04	12.3 ± 0.5	1425.3 ± 30.7
60:40	22.4	Fail	47.10± 2.91	7.5 ± 0.2	128.5 ± 12.3
40:60	30.6	V-2	103.33± 5.76	4.2 ± 0.1	23.5 ± 2.5

2.5 Effects of Radiation on Polymers

Radiation can be produced by various method, they can be produced by nuclear reactors or found in radioactive wastes. Radiation can be in many forms such as electromagnetic waves: gamma, or as particles such as alpha, beta, positrons, high energy electrons and neutrinos. Interaction mechanism like collisions with nuclei and electron striping of particles caused most of the particles to be attenuated in close proximity of the vicinity of the fuel elements (Glasstone and Sesonske, 1981 cited in Kulshreshtha and Vasile, 2002). Secondary radiations will be induced and are emitted in the form of recoil protons heavy ions, and x-rays. Fast photons and thermal neutrons have higher penetration power and are able to interact with particles that are far from the reactor core through mechanisms characteristic of their respective types of radiation. The fast photons and thermal neutrons are responsible for the most of the noticeable changes in polymers (Kulshreshtha and Vasile, 2002).

The physical and chemical properties of polymers can be altered by the irradiation treatment in the form of X-rays, electron beams, and gamma rays.

Radiation exposure will produce both transient and permanent changes in polymer. Transient behaviour is observed through the induced electrical conductivity in polymer where radiation will cause permanent change in the chemical structure of the polymer. Radiation transfers energy to the polymer molecules as a result “excite” the electrons to a higher energy state causing partial decomposition of molecules, reactive groups or radicals. These groups are then abled to react with each other to form new chemical arrangement. Irradiation can initiate polymerization, grafting, crosslinking and chain scission reactions. Crosslinking is where two long polymer chains with an extra valence linked to produce a new network. This usually increases the molecular weight of the polymer. Another example is the scission of chain, where the degradation of the polymer chain into a shorter chain network (Makuuchi and Cheng, 2012).

Other uses of radiation on polymer are sterilization of medical products, curing monomeric coatings and inks which are the work of the early developments. Some of the practical uses of radiation on polymeric materials are to produce heat-shrinkable plastic films for food packaging or encapsulations for industrial products, plastics foams and others. Radiation-cured inks are used for printing such as newspapers and magazines or other packaging products. Industrial irradiation processes use high energy electron accelerators have high throughput rates and the costs for each unit product are more competitive compared to conventional chemical processes. High energy irradiation allows rapid changes in the products which are useable immediately after processing (Cleland, Parks and Cheng, 2003). Different dosage of radiation will induce different effect onto the polymers. It is known that the dose required to obtain desired and beneficial effects is lower in higher molecular weights materials (Charlesby, 1977).

2.5.1 Photon Interactions

Gammas and X-rays are photons that ionise atoms, through three main processes (Kroschwitz, 1988). The first process is in low energy photons (<0.05 MeV), where the photoelectric effect is predominant, amounts the total energy transfer of photon’s

energy to the electrons in the inner cells which are closest to the nucleus. As energy is transferred, electron in the inner cell is ejected from the atom which becomes ionised. This process is followed by the rearrangement of the remaining electrons within the cells, which causes the emission of x-rays electrons. The next mechanism is the Compton scattering effect which is also predominant for photon with lower energy (0.1-10 MeV). In this process, the incident photon collides onto one of the atom's electrons, most likely to those situated on the valence shells and ejects the electron from the atom. As the photon collides at the valence cells, the photons, now in reduced energy, will move in directions that are different from the incident direction. Both the photon and stripped electron may absorb sufficient energy to ionise several more atoms. The last mechanism is pair production mechanism, suitable for photon's energy equalling to or greater than 1.022 MeV. This process occurs in the vicinity of a heavy nucleus and causes the disappearance of the incident photon leading to the creation of an electron-positron pair. The photon and electron are emitted in opposite directions and ionising more atoms. The three interaction mechanisms results in a rather uniform photon energy deposition within the irradiated polymers, such as organic polymers where the Compton scattering effect is predominant for photon below 2.5 MeV energy level (Kulshreshtha and Vasile, 2002).

2.5.2 Neutrons Interactions

Fast (1-2 MeV) and thermal (0.0253 eV) neutrons and atoms interactions are more complicated than that of Photon Interactions. The neutrons have neither neutral electric charges, nor positive or negative. The neutrons are not technically ionising radiation, but in practice they are. The ionisation is initiated by the recoil charged protons from inelastic and elastic collisions between the neutrons and light nuclei through a knockout process. Protons, energetic charged ions, having higher ionising power than electrons, will cause higher damage from the incident neutrons. Furthermore, the fast and thermal neutrons may be absorbed, through nuclear reaction, into the atoms nuclei that are transmuted into radioactive isotopes. These radioisotopes will undergo radioactive decay which will emit beta and gamma

particles. The duration of induced radioactivity depends on the type of atom present in the irradiated polymer. For most of the polymers, the majority atoms presents are that of: such as carbon, oxygen, nitrogen and hydrogen. These atoms have a low neutron absorption cross section or short the activation products live. As a result, the activation process presents to be a primary concern only if impurities (mostly metallic) are found in significant quantities. The overall effect of the neutrons interactions can be summarised as high ionisation powers of recoil protons and ions concentrating damages along specific tracks and in more localised sites (Kulshreshtha and Vasile, 2002).

2.5.3 Crosslinking and Chain Scission of Polymers

Crosslinking is one of the most important effects produced by polymer irradiation due to the improved mechanical and thermal properties of the irradiated polymers. Crosslinking and chain scission will occur simultaneously during radiation treatment with either one predominates (Charlesby, 1960). The density of crosslinking *(G(X))* and chain scission *(G(S))* is given by the G-value. G-value is given the number of events (yield) per 100 eV of radiation absorption. As 1ev is equivalent to 1.602×10^{-19} kGy ·g, 100 eV is equivalent to 1.602×10^{-17} kGy ·g. Ratio of *G(S)/G(X)* below 1.00 favours crosslinking, therefore polymer with high *G(X)* and low *G(S)* is preferable. The value of *G(X)* for crosslinking and *G(S)* for chain scission will change respectively to the received radiation dosage. It is commonly known that value of *G(S)* will increase more than *G(X)* with increasing dose which suggested that at a certain dosage the *G(S)* will dominate over *G(X)* for an initially crosslinked polymer. In general, polymers with low *G(S)/G(X)* value are able to withstand high dose without excessive degradation. For example, polystyrene has 0.41 of *G(S)/G(X)* and its tolerance dose range from 800 to 30 000 kGy, while polymers with big benzene rings also tend to have higher radiation stability. This is due to the rings ability to absorb and dissipate energy without bond disruption (Parkinson and Sisman, 1991). Generally, crosslinking is greater in high energy electron beam compared to low energy gamma ray and X-ray because at lower dose rate, longer duration of treatment will allow more oxidation to occur (Cleland, Parks and Cheng, 2003).

As mentioned that radiation effects will change the polymer molecular weight. The radiation effects on molecular weight can be measured quantitatively:

$$^{1}/_{Mn} = {}^{1}/_{Mn,\,o} + [G(S) - G(X)]D/100NA \qquad \text{(E 2.7)}$$

where

Mn = number average molecular weight of exposed polymer, mole

Mn,o = initial average molecular weight, mole

D = received dose, kGy

NA = Avogadro's number, $6.02214129 \times 10^{23}$ mol^{-1}

Although chain scission is not favourable in most of the industry applications but it is useful to reduce the molecular weights of the polymer when required. For example, polytetrafluoroethylene (PTFE) has low *G(X)* and high *G(S).* Therefore irradiation will induce reduction of molecular weight. The reduction of molecular weight is useful in the industry to turn scraps of PTFE into finer particles because untreated PTFE is very tough and slippery to be able to grind. Degradation of PFTE will make it readily to be grinded (Derbyshire, 1980).

The physical properties of a polymer under radiation treatment depend on the degree of crosslinking and chain scission. Crosslinking will lead to an increase in modulus and decrease the elongation of polymer while degradation (chain scission) will cause reduction in modulus and strength (Bopp and Sisman, 1953 cited in Miller, 1959, p.774). The direction of radiation effect is primarily affected by the changes in the chemical structure of the polymer. For example, polyethylene and polybutadiene, with low *G(S)/G(X)* ratio, is crosslinked while polyisobutylene and polytetrafluoroethylene are, with high *G(S)/G(X)* ratio, is degraded (Cleland, Parks and Cheng, 2003). In a particular class of vinyl polymers:

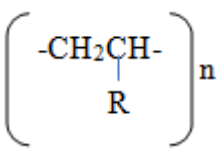

Figure 2.5: Vinyl Polymers Chemical Structure

in which crosslinking is shown to be predominant with the main-chain constituted of carbon bonds. In contrast, the chain scission is predominant as the tertiary hydrogen is replaced by a methyl group:

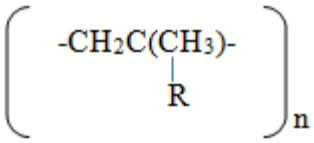

Figure 2.6: Vinyl Polymer Chemical Structure

Looking from the standpoint of radiation resistance, both crosslinking and degradation are undesirable because crosslinking will lead to the embrittlement of the polymer while chain scission will cause softening and loss of strength in the polymer. If the radiation induces only crosslinking or chain scission in a polymer, it is undesirable because the polymer properties will be of extreme (very soft or very brittle). Even though one of the reactions is predominant in certain polymers, the properties are more desirable with the simultaneous occurrence of both reactions in polymers, to create a product of an intermediate or moderate property between brittle and soft. As stated previously that aromatic groups has higher radiation stability, this stability has been well established on a quantitative basis. In polyethylene, the energy required for it to produce crosslink is about 25 to 30 eV. While in polystyrene, the energy required is as high as at least 500 eV, which is 20 times greater than that of polyethylene (Shultz, Roth and Rathman, 1956 cited in Miller, 1959, pp.775). It is also found that radiation process in the presence of oxygen will create competition for the polymer molecules to crosslink. The oxygen may diffuse into the polymer and alter the radiation effect or suppress the crosslinking and cause oxidation instead.

2.5.4 Specific Energy Requirement

Specific energy requirement is proportional to the absorbed dose (*D*) by the irradiated polymer. The definition of the common dose unit states that 1 kilogray (kGy) equals to 1 kilojoule (kJ) of absorption, or 1 kilowatt second per kilogram (kWs/kg) of material. Thus, the specific energy equation is stated as follow:

$$SE = D \quad \text{(E 2.8)}$$

where

SE = specific energy, kJ/kg

D = kGy

Whereas the *SE* expressed in molecular weight and G-value are stated as follow:

$$SE = 6.022 \times 10^{23} \times (100/G) \times 1.602 \times 10^{19}/10^{3} \quad \text{(E 2.9)}$$

$$SE = 9.65 \times 10^{3}/G \quad \text{(E 2.10)}$$

where

SE = specific energy, kJ/mole

$$SE = 9.65 \times 10^{6}/G \times (\text{Molecular Weight}) \quad \text{(E 2.11)}$$

where

SE = specific energy, kJ/kg

Combining (E 2.8) to (E 2.9) the following equation is obtained:

$$D = 9.65 \times 10^{6}/G \times (\text{Molecular weight}) \quad \text{(E 2.12)}$$

where

D = kGy

Take for example a polymer with molecular weight of 1000 with G-value of 1, the dose required to convert or induce chemical changes in all the molecules in the polymer would be around 9650 kGy. The G-value is commonly range between 0.1-10 for most polymers. Therefore the molecular weights are the significant factor influencing the dose required. When a polymer requires radiation at extreme dose for example,10,000 kGy, the process would be impractical due to the high processing cost and high energy requirement. Applying such high radiation dose may cause

decomposition in the polymers due to the high temperature applied on the polymer if the process is conducted without cooling. Radiation supplies energy and some of the energy will convert into heat energy. Temperature rise in irradiated polymer is proportional to the *SE* and *D*. The difference in temperature can be calculated using the following equation (Cleland, Parks and Cheng, 2003):

$$\Delta T = D/c \qquad \text{(E 2.13)}$$

where

T = temperature, K

D = is the average dose, kGy

c = specific heat capacity, J/g·K

2.5.5 Electron Beam Interactions

Radiation using fast electrons, the energy transferred to the molecules of the polymer will results in ionisations and excitations of the molecules. Once the energy is absorbed, the polymer molecules will give rise to free radicals, which are responsible for the chemical transformations found in polymers (Czvikovszky, 1996). The main effects of electron beam irradiation (Burger, et al., 1997) are crosslinking, chain scission and oxidation. Radiation usually causes structural changes in most of the polymer materials.

The chemical structures influence the type of reaction that is dominant in different polymers under electron beam irradiation. Some of the electron beam irradiated polymers are discussed. The PVC/epoxidised natural rubber (ENR) blends produces radiation-induced crosslinking under electron beam bombardment enhanced the mechanical properties of the blends. Both pelletised polybutylene succinate (Bionolle) and powdered polypropylene-co-ethylene (CPP) have been submitted to heavy radiation treatment, even at relatively low irradiation dose (D < 100 kGy), the tensile strength and elongation at break are reduced dramatically. One of the possible methods to prevent the negative effect of ionising radiation is to add

some reactive groups to transfer energy and intermolecularly dissipate the energy. These reactive groups act as an energy sink. However the polymers properties have to be maintained while adding such reactive groups (Ivanov, 1992). According to the CPP/Bionolle blend case, the energy sink is the pelletised polypropylene grafted maleic anhydride (Modic), it has a cyclic anhydride group. High energy electron beams are first used for sterilization of medical equipment, curing of coating or composites. Electron beam is more suitable to curing process as it is more controlled instead of thermal curing. Electron beam curing is a rapid non-thermal process which applies highly energetic electrons at controlled doses. Irradiation usually causes either polymerisation or crosslinking of polymers. Electron beam curing takes place at either ambient and/or sub-ambient temperatures. This irradiation method has advantages over conventional autoclave curing such as highly reduced curing time, utilization of low cost tooling materials, reduced energy consumption, leading to order of magnitude improvements in throughput, control over curing energy absorption profile and, reduced volatiles emissions. Electron beam cured polymers have shown to present excellent mechanical properties, high glass transition temperatures and low void content. In Raghavan (2008) work, he found that for an epoxy reinforced with IM7 carbon fibre, that prolonged exposure in lower dose rate will produce higher cure than those exposed to shortened exposure in higher dose rate. However, the latter give rises to a higher T_g and mechanical properties. Electron beam pretreatment of polymers (such as PE) is a very useful technique to obtain a functionalised polymeric surface as it is possible to bond the treated surface to the inorganic fillers and other plastic materials. Stronger and tougher PE materials can be obtained by functionalising PE being treated with heavy electron beam. The technique has provided significant enhancement on the compatibility of PE with inorganic filler (Guan, 2000).

CHAPTER 3

METHODOLOGY

3.1 Material Used

In order to conduct this research, two materials were used namely alumina trihydrate (ATH) and acrylonitrile-butadiene-styrene (ABS). The specifications of these chemicals were discussed in the following sections.

3.1.1 Acrylonitrile-Butadiene-Styrene

The grade of ABS polymer that would be used as the base material for this study was Toyolac 700 314, manufactured by Toray Plastics Malaysia Sdn Bhd. This is a general purpose ABS resin with a specific gravity of 1.05 g/cm^3. The quoted composition of the ABS is 95 % or more of ABS copolymers and 5 % or fewer additives.

3.1.2 Alumina Trihydrate

The grade of ATH fillers that were used in this study was flame retardant grade, manufactured by Chung Chemicals Sdn Bhd with particle size of 20 microns. The specific gravity is 2.42 g/cm^3.

3.2 Samples Preparation

3.2.1 Compounding

The ABS resins and ATH powders were compounded using Nanjing Giant SHJ-20 Twin-Screw Extruder with an L/D ratio of 32:1 fitted with a two-strand die. The formulations of the samples were compounded as tabulated in Table 3.1.

Table 3.1: The Composition of the Samples

Label	ATH (phr)
ABS-60	60
ABS-80	80
ABS-100	100
ABS-120	120
ABS-140	140

ATH powder and ABS resin were mixed and agitated homogeneously before pouring into the extruder. The ABS composites were compounded at 180 ^{o}C with screw speed of 100 rpm for 12 min. The resultant composites strands were cooled in ambient air before entering a pelletizing hopper unit where the composite strands were cut into pellet form.

3.2.2 Compression Moulding

The compounded samples were compression moulded into sheet with dimensions of 15 cm x 15 cm x 0.1 cm using a YX-1200 model hot press machine. Initially, the compounded samples were preheated in the hot press machine at heating temperature of 170 ^{o}C for 5 minutes. After that, the pre-heated sample was compressed with pressure of 10 MPa at heating temperature of 170 ^{o}C for 5 minutes. After 5 minutes, the sample was cooled down to room temperature with cooling rate of 20 ^{o}C/ min under pressure of 10 MPa for another 2 minutes.

3.2.3 Irradiation Process

The samples in 1 mm thickness sheet were electron beam irradiated with EPS-3000 electron beam machine. Irradiation were conducted using beam current of 5 mA and energy of 1.5 MeV. The samples were irradiated with dosages of 50 kGy, 100 kGy, 150 kGy, 200 kGy and 250 kGy with 50 kGy irradiation dosage per pass to avoid surface heating. The irradiation process were carried out under ambient conditions.

3.3 Characterization Test

3.3.1 Tensile Testing

The tensile test was carried out to investigate the tensile properties of the samples under loading. The 1-mm thick sheets were cut into dumbbell shape according to the ASTM D1822 by using Instron 5848 micro tester. The samples were examined under a load of 5 kN with a crosshead speed of 50 mm per minute. The gauge thickness of the samples was measured before carrying out the tensile testing. The tensile strength, elongation at break and young modulus of samples were recorded and an average value of five samples was taken.

3.3.2 Flammability Test

The flame retardancy of the ATH added ABS samples were investigated and tested by using limiting oxygen index test (LOI). The 1-mm sheets were cut into the dimensions of 150 x 50 x 1mm^3 and the cut specimen was placed in a vertical position at the center of a transparent test column. Measurements were taken in accordance with ASTM D2863. A mixture of nitrogen and oxygen gases were supplied and purged into the transparent test column to form a homogenous oxygen-nitrogen atmosphere inside the test column. The upper end of the specimen was ignited with a gun burner. The concentration level of oxygen gas in the mixture was

adjusted until it was sufficient enough to support the combustion of specimen. Nine specimens would be tested per each formulation.

3.3.3 Microstructural Property Assessment

JEOL model JSM-6301F field emission scanning electron microscope was used to examine the dispersion of the fillers and the SAN matrix at magnification of x1000, x8000 and x15,000 with accelerating voltage of 15.0 kV. The fractured surface of samples was cut into a 2mm x 2mm dimension. The cut samples were mounted onto a copper stub with the fractured surface facing up. Prior to the SEM analysis, the mounted samples were sputter coated with a thin gold layer that would provide a good conducting flow.

3.3.4 Gel Content Test

The measurement of gel content of the samples were carried out in accordance to ASTM D2765. The samples were gravimetrically immersed and heated in methyl ethyl ketone at heating temperature of 80 ℃ for 24 hours of extraction. After 24 hours, the samples were then rinsed with clean xylene for at least 4 times to remove the remaining of soluble materials on the extracted samples. After the cleaning, the samples would be completely soaked with methanol for 20 minutes and then dried to a constant weight in a vacuum oven for 5 hours. The gel content was measured using the following equations:

$$Gel\ Content\ Percentage\ (\%) = (W_1 / W_2) \times 100\ \% \qquad \text{(E. 3.1)}$$

where,

W_1 = weight after extraction, g

W_2 = initial weight, g

CHAPTER 4

RESULTS AND DISCUSSIONS

4.1 Gel Content Test

Gel content test was conducted to determine the degree of crosslinking formed in ABS matrix when subjected to various irradiation dosages. Figure 4-1 illustrates the gel content of all AHT added ABS samples under various electron beam irradiation dosages. According to Figure 4.1, the gel content of all non-irradiated ATH added ABS samples did not show a zero value. This indicates that the non-irradiated ATH added ABS samples did not completely dissolve into hot solvent (MEK) after 24 hours of extraction process. Furthermore, increasing of ATH loading levels from 60 phr to 140 phr was also found to gradually increase the gel content value of non-irradiated ABS composites. This might be due to the occurrence of ATH particles in ABS matrix which could significantly weaken the solubility of ABS matrix into hot solvent for 24 hours of extraction process. The crystalline structure of ABS matrix might have the ability to resist dissolving by MEK solvent. The studies conducted by Bee, et al. (2014) and Sun, et al. (2014) showed that crystallinity had significant effect in the solubility of polymers matrix.

As seen in Figure 4.1, the increment in the irradiation dosage from 0 kGy to 100 kGy significantly increased the gel content of 60 phr to 120 phr ATH added ABS composites. This implies that the ABS matrix is much more difficult to dissolve in MEK solvent due to the formation of cross-linking network. The electron beam irradiation caused the formation of polymeric free radicals in the ABS matrix which induced the crosslinking of polymer chains (Lee, et al., 2013). The further increment

in irradiation dosage (150 kGy) reduced the gel content for ATH added ABS composites of 60 phr to 120 phr. This shows that high irradiation dosage generated excessive amount of polymeric free radicals which would lead to chain scissioning predominating over crosslinking. High amount of irradiation induced chain scissioning is undesirable because polymer may degrade due to either a backbone main-chain scission or hydrogen abstraction (Ng, et al., 2014). As the irradiation dosage increased further (200-250 kGy), the gel content value for ATH added ABS composites from 60 phr to 120 phr was subsequently increased. This cleaved polymer chains generated by irradiation-induced chain scission had absorbed the energy to facilitate crosslinking. This can be proven by the approximate similar gel content value of prior to and after the chain scission. However increment in irradiation dosage had insignificant effect on the gel content of ATH added ABS composites at 140 phr. The deterioration in this efficacy was due to the interruption of ATH particles in the mobility of polymer chains in the ABS matrix. The presence of excessive ATH particles deteriorated the polymeric free radicals mobility to form bonding with other polymer chains thus contributing to the low increment in gel content of approximately 11 %.

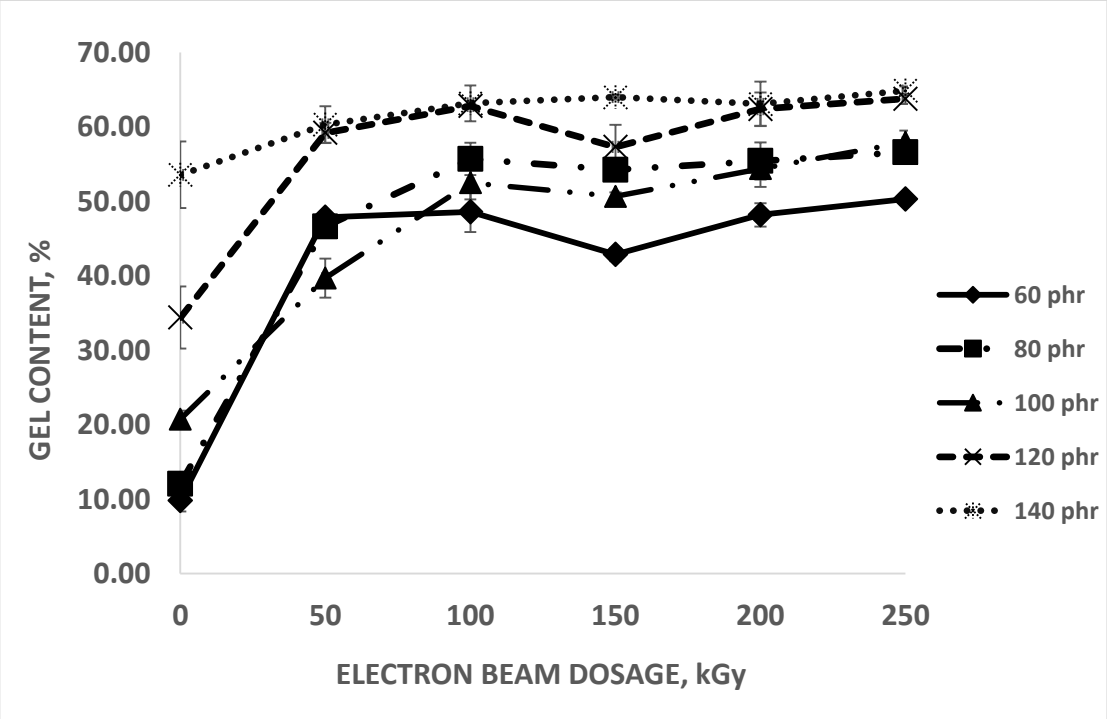

Figure 4.1: Influence of Electron Beam Dosage on the Gel Content of ATH added ABS with Increasing ATH Loading Level

4.2 Mechanical Properties

4.2.1 Tensile Test

The effect of loading level of ATH and irradiation dosage on the tensile strength of ATH added ABS composites is shown in Figure 4.2. As expected, the presence of ATH induced decline in the tensile strength. By referring to Figure 4.2, the tensile strength of all non-irradiated ATH added ABS composites gradually decreased with increasing loading level of ATH. This might be due to the poor interfacial adhesion between ATH particles and ABS matrix caused by agglomeration. ATH particles are material that will likely to agglomerate in a polymer matrix (Zhang, et al., 2005) thus the agglomeration of ATH particles would cause poor dispersion of ATH particles in ABS matrix. Poor dispersion of ATH particles would cause poor alignment of polymer chains where the polymer chain could not arrange itself side by side. According to Murray, et al. (2013) irregular alignment of polymer chains would lead to the formation of voids in the ABS matrix. Furthermore the large aromatic found in ABS would also contribute to the formation of void because it is large in size inducing low crystallinity in ABS matrix. The voids formed would act as stress concentrator points and caused poor stress transfer in the ABS matrix when subjected to stretching (Wang, et al., 2014).

As shown in Figure 4.2, at low loading level of ATH (≤80 phr), the tensile strength of ATH added ABS composites increased with increasing irradiation dosage from 0 kGy to 100 kGy. When subjected to irradiation, the interfacial adhesion of ATH particles and ABS matrix was enhanced due to the formation of crosslinking. Crosslinking converted the linear molecular structure into a three-dimensional network by generating polymeric free radicals which bond with other polymer chains. The network formed would reduce the mobility of polymer chain to dislocate enhancing the ability to resist crack propagation thus improving the tensile strength (Baillet and Delfossem, 1990). Furthermore, the increment in crosslinking would increase the molecular weight of the polymer chains and also would formed a stronger intermolecular bonding of ATH added ABS composites thus improving the tensile strength. However, the tensile strength of ATH added ABS composites decreased with further increment in irradiation dosage (150-200 kGy). This is in

accordance with the result obtained in gel content test where the irradiation-induced chain scission had also occurred at 150 kGy. The irradiation-induced chain scission could attribute to the decreasing of tensile strength as the ABS backbone chain might be broken by the high energy bombardment. This would reduce the length of the ABS chain where and subsequently reduced the tensile strength. As further irradiation was introduced (250 kGy) it was observed that the tensile strength of ATH added ABS composites had increased marginally. The tensile strength of ATH added ABS composites at 250 kGy was higher than 200 kGy but it was slightly lower than 100 kGy which could be attributed by the slight increase in gel content value.

According to Figure 4.2 at high loading level of ATH (≥100 phr), application of irradiation dosage increment from 0 kGy to 100 kGy had insignificant effect on the tensile strength of ATH added ABS composites. This might due to the deterioration of polymeric free radicals mobility as the amount of ATH particles were in excessive and interfered the movement of the polymeric free radicals in the ABS matrix. Thus, the intensity of the formation of crosslink network was low. Figure 4.2 shows that the tensile strength gradually reduced as the irradiation dosage increased further (150-250 kGy). This clearly indicates deterioration of ABS matrix despite the marginal increment in gel content value as shown in Figure 4.1. The deterioration in tensile strength might be attributed to the low crystallinity and the formation of voids generated by crosslinking. Such voids acts as weak point in thte material and promote crack propagation reducing the load required to break the polymer (Mapkar, 2008). With every addition application of irradiation dosage on the polymer, the arrangement of the polymer chains would realign itself and thus deteriorating the crystallinity of polymer chains further. Therefore the increment in crosslinking after irradiation dosage of 150 kGy would not improve the tensile strength of ATH added ABS composites.

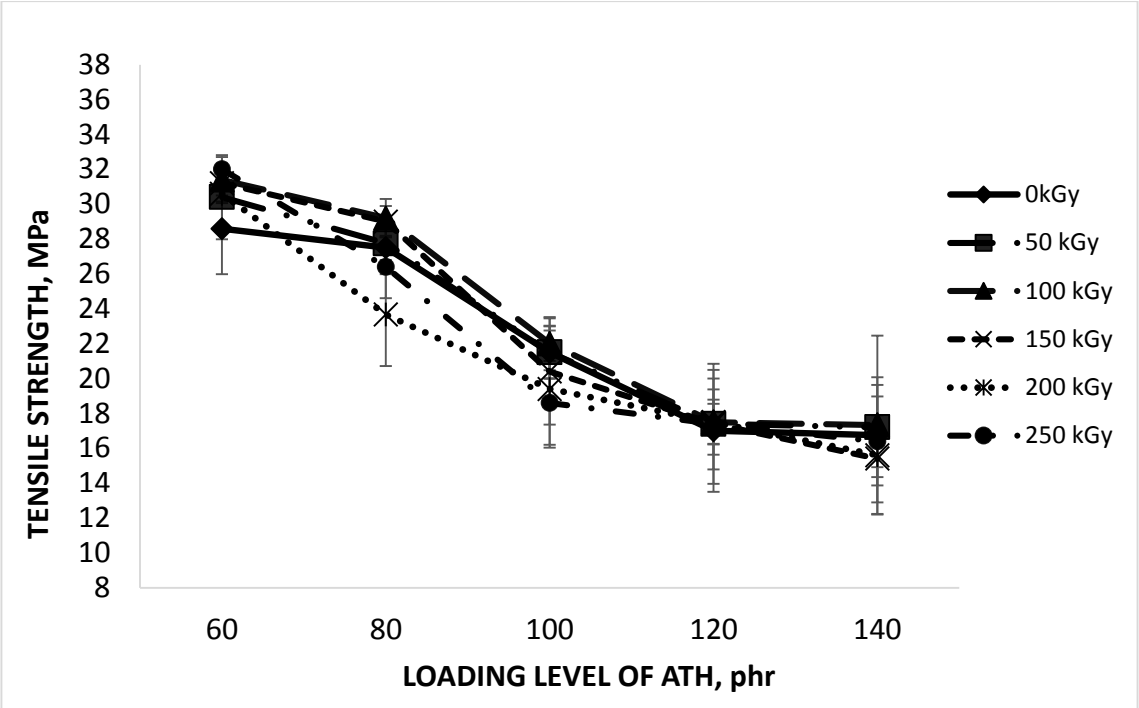

Figure 4.2: Influence of Loading Level of ATH on the Tensile Strength of Electron Beam Irradiated ATH added ABS

4.2.2 Elongation at Break

By referring to Figure 4.3, for non-irradiated ATH added ABS (0 kGy), the elongation at break gradually decreased with increasing loading level of ATH from 60 phr to 140 phr ATH. This was because the increasing amount of agglomeration caused by increasing loading level ATH significantly restricted the mobility of polymer chains and therefore the polymer chain resisted deformation. The formation of voids would also contribute to the low elongation at break because the stress would concentrate on the voids causing the breaking of polymer chain much easier. As for ATH added ABS composites of low ATH loading level (≤80 phr), the elongation at break decreased with increasing irradiation dosage. This was because the crosslinking occurred would increase the entanglement of the polymer chains network deteriorating the ability of the polymer chain to slide in the matrix. In addition, chain scission would generate a greater amount of shorter chains which reduced the distance that the polymer chains could slide past each other during

straining and thus lower the elongation (Ng, et al., 2014). As for the ATH added ABS composites at high loading level (≥100 phr) the increasing irradiation dosage had insignificant effect on the elongation at break. This could prove that the high loading level of ATH acted as strong obstacles which would cause immobility of the polymeric free radicals formed thus preventing the formation of crosslink network. Furthermore, the formation of shorter polymer chains would also anchored to its position after chain scission due to the high amount of ATH particles. Therefore the difference elongation at break maintained at an approximate average of only 0.375 %.

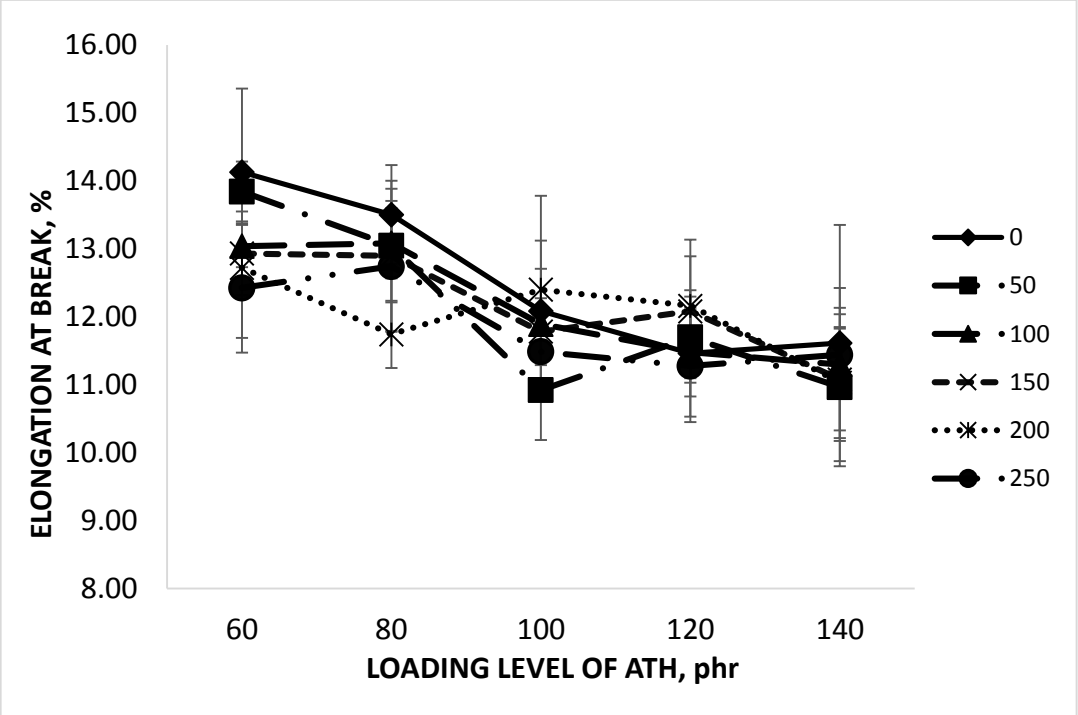

Figure 4.3: Influence of Loading Level of ATH on the Elongation at Break of Electron Beam Irradiated ATH added ABS with Different Irradiation Dosage

4.2.3 Young Modulus

As shown in Figure 4.4, for non-radiated ATH added ABS composites, the young modulus increased with increasing loading level of ATH from 60 phr to 100 phr. The increased amount of ATH particles in the ABS matrix, caused the ABS matrix to be less prone to the slip dislocation of polymer chains thus leading to higher young

modulus. However the young modulus for the ATH added ABS composites reduced with increasing loading level of ATH from 120 phr and 140 phr. This indicated that the amount of ATH particles had been excessive which might have disrupted the recrystallization of polymer chain in ABS matrix during sample processing. Irregular recrystallization of polymer chains might cause the formation of short polymer chains. The shorter polymer chains have higher mobility and could deform under lower loading when stretching was applied which subsequently increased the plastic deformation of ABS matrix (Liu, et al., 2012).

By referring to the Figure 4.4 at irradiation dosage of 50 kGy for 60 phr ATH added ABS composites, the young modulus increased from 153.78 MPa to 571.10 MPa. The great increment of modulus indicated that the introduction of crosslinking increased the intermolecular bonding by creating a three-dimensional network from linear polymer structure (Tillet, Boutevin and Ameduri, 2011). The reduction in mobility of the three-dimensional network would require a greater amount of strength to stretch the composites. However as further ATH loading level was introduced (80-140 phr), the young modulus reduced with increasing loading level of ATH. This shows that the incorporation of ATH particles might have weakened the interfacial adhesion of the ATH particles and ABS matrix which would lead to the formation of agglomeration. The formation of agglomeration would cause discontinuity in the ABS matrix leading to formation of shorter chains during sample processing (compounding and compression moulding) and subsequently increased the plastic deformation of ABS matrix. As seen in Figure 4.5 irradiation had insignificant effect on young modulus for all ATH added ABS composites formulations when subjected to further irradiation dosages (150-250 kGy). This could due to the formation of short polymer chains caused by irradiation-induced chain scission. The formation of short polymer chains would have less restriction from crosslinking network and thus requiring lower loading for stretching.

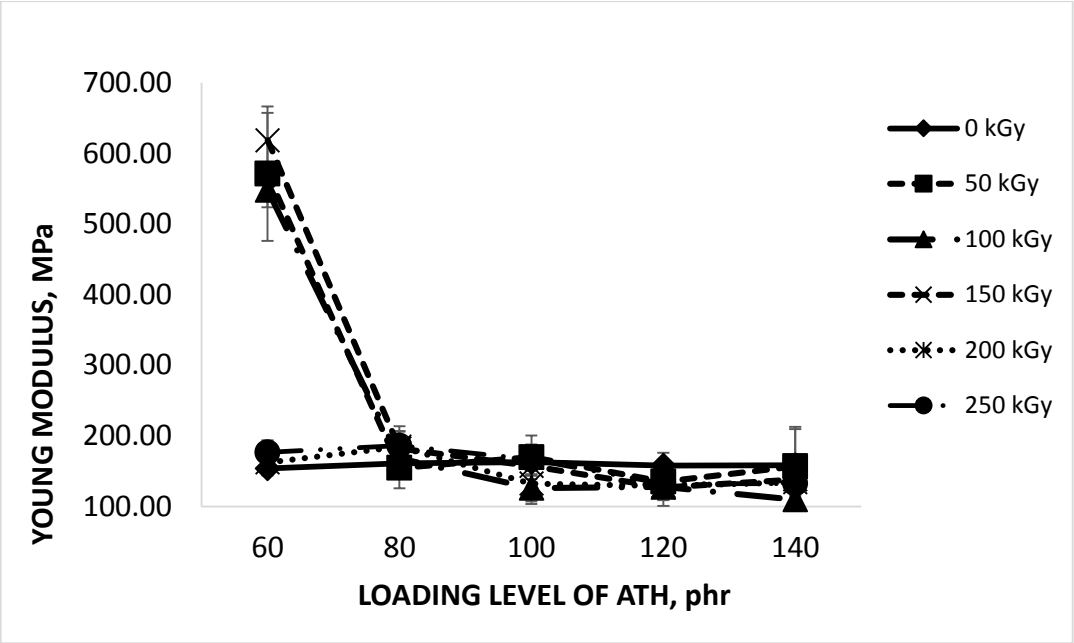

Figure 4.4: Influence of Loading Level of ATH on the Young Modulus of Electron Beam Irradiated ABS

4.3 Scanning Electron Microscopy (SEM)

Figure 4-5 illustrates the SEM images of non-irradiated ATH added ABS. As seen in Figure 4-5(a), the ATH homogenously disperse in ABS matrix and the surface was smooth and had a brittle nature (Cui, Guo and Chen 2007). The smooth surface morphology attributes to good compatibility of ATH and ABS. In Figure 4-5(b and c) the bright white parts are the agglomerates of ATH particles within ABS matrix. The rough surface shows the incompatibility of ATH particles and ABS matrix while the bubble voids formed are caused by volatiles produced by ABS during sample preparation (Wang, et al., 2014). The intensity of bubble voids increased as observed in Figure 4-5(d and e). The morphology of non-irradiated sample as shown in Figure 4-5 is in agreement with the tensile strength results observed in the morphology.

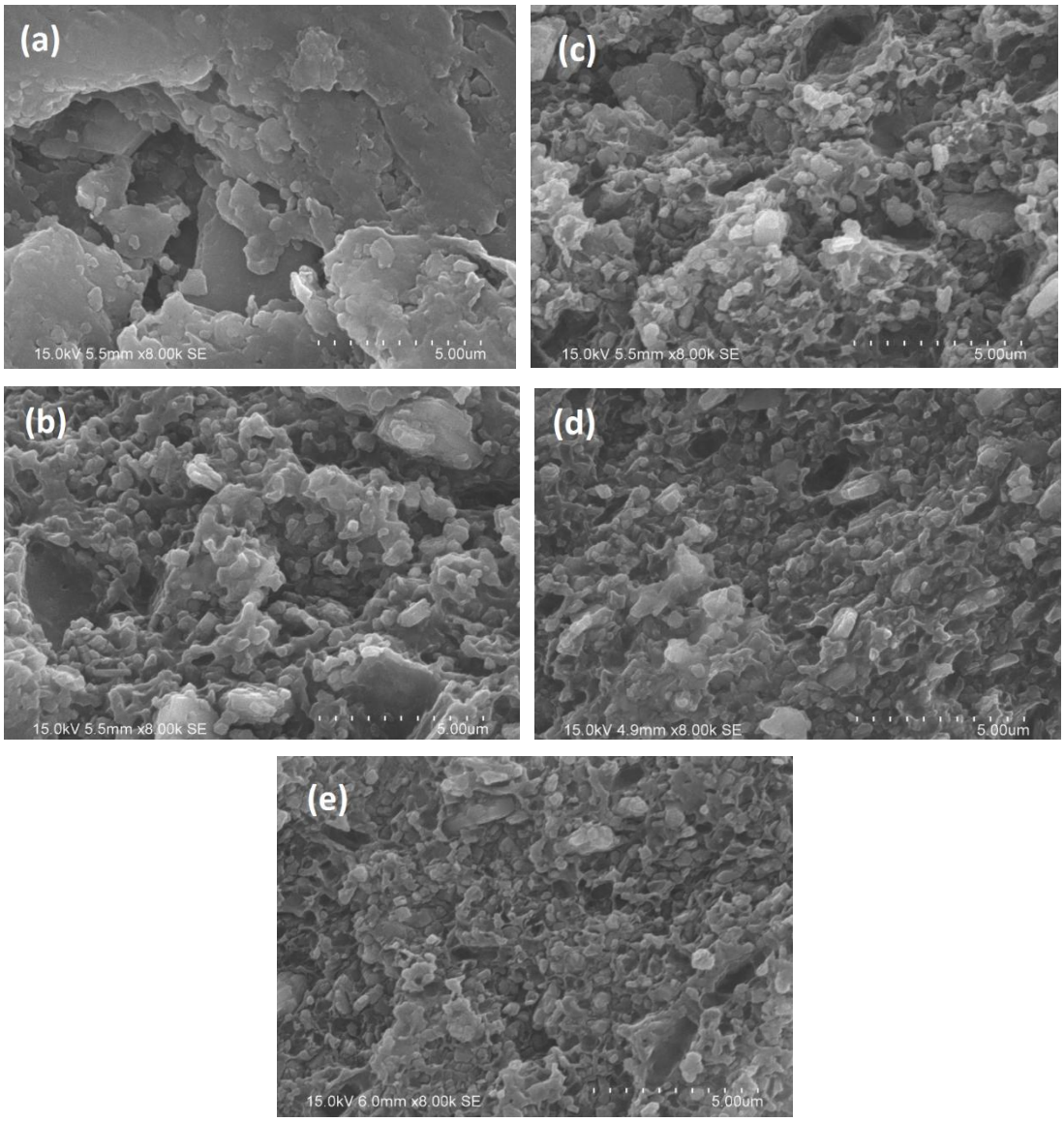

Figure 4.5: SEM Images of Fracture Surface of ATH added ABS Composites with Loading Level of (a) 60 phr, (b) 80 phr, (c) 100 phr, (d) 120 phr and (e) 140 phr

Figure 4-6(a and d) shows the SEM images of low ATH loading level at low irradiation dosage. The morphology for both of the ATH added ABS composites formulation is relatively similar where a great amount of bubble voids and agglomeration can be observed. Figure 4-6(a) however, has a better continuity of the ABS matrix and has voids that are smaller in size compared to Figure 4-6(d). Therefore the tensile strength of 60 phr ATH added ABS composites in Figure 4-6(d) should be better than the 80 phr in Figure 4-6(d). The morphology observed supports

the findings in the tensile strength. Figure 4-6(b and c) and Figure 4-6(e and f) show the SEM images of high irradiation dosage for low ATH loading level. The morphology of the ATH added ABS composites is similar regardless of the increasing irradiation dosage. It can be observed that there are many bubble voids and agglomerates which attribute to low tensile strength. Furthermore, the surface shows flakes; a small irregular sea-island size which attribute to the brittleness of the ATH added ABS composites. The elongation at break and young modulus are small because the ATH-ABS interfacial adhesion had been weakened by the excessive amount of bubble voids and agglomerates.

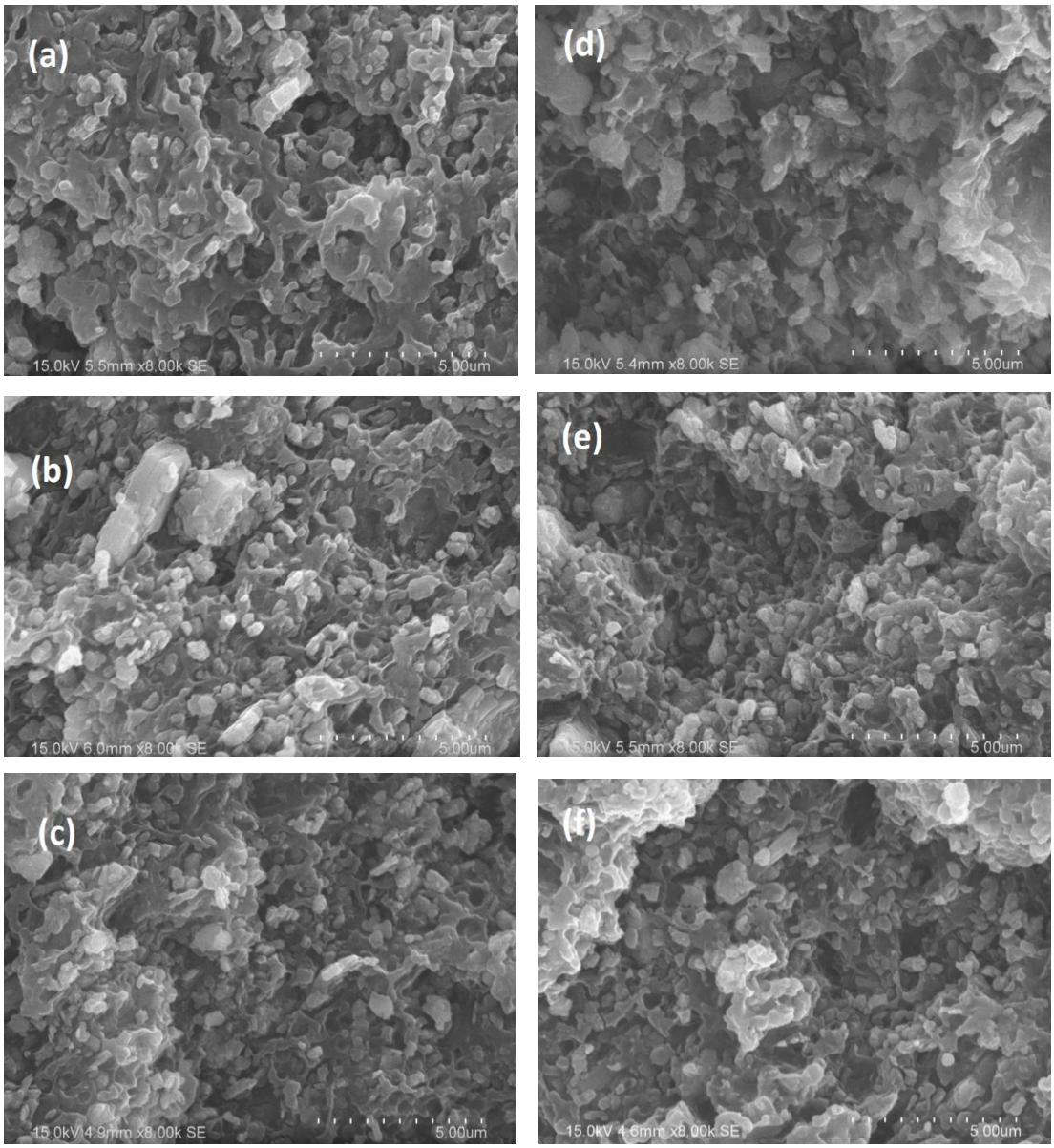

Figure 4.6: SEM Images of Fractured Surface of 60 phr (a) 50 kGy, (b) 150 kGy, (c) 250 kGy and 80 phr (d) 50 kGy, (e) 150 kGy, (f) 250 kGy.

Figure 4-7(a and d) show the morphology of high loading level of ATH at low irradiation dosage. The ATH disperse homogenously with ABS in small agglomerates. The morphology shows degradation of ABS matrix and the ABS matrix deformed easily as shown in the presence of flakes thus having low elongation at break and young modulus as well as tensile strength. The loading level of ATH has been excessive which degraded the mechanical properties of ATH added ABS composites. Similar morphology is observed for ATH added ABS composites of high ATH loading level at high irradiation dosage as shown in Figure 4-7 (b and c) and Figure 4-7 (d and e). Therefore the variations of value for the mechanical properties are relatively small. In Figure 4-7(c and f), the circled part clearly shows the trails of large ATH particle agglomerates which could not be seen in Figure 4-7(b and e). This could attribute to the reduction in tensile strength from 150 kGy to 250 kGy.

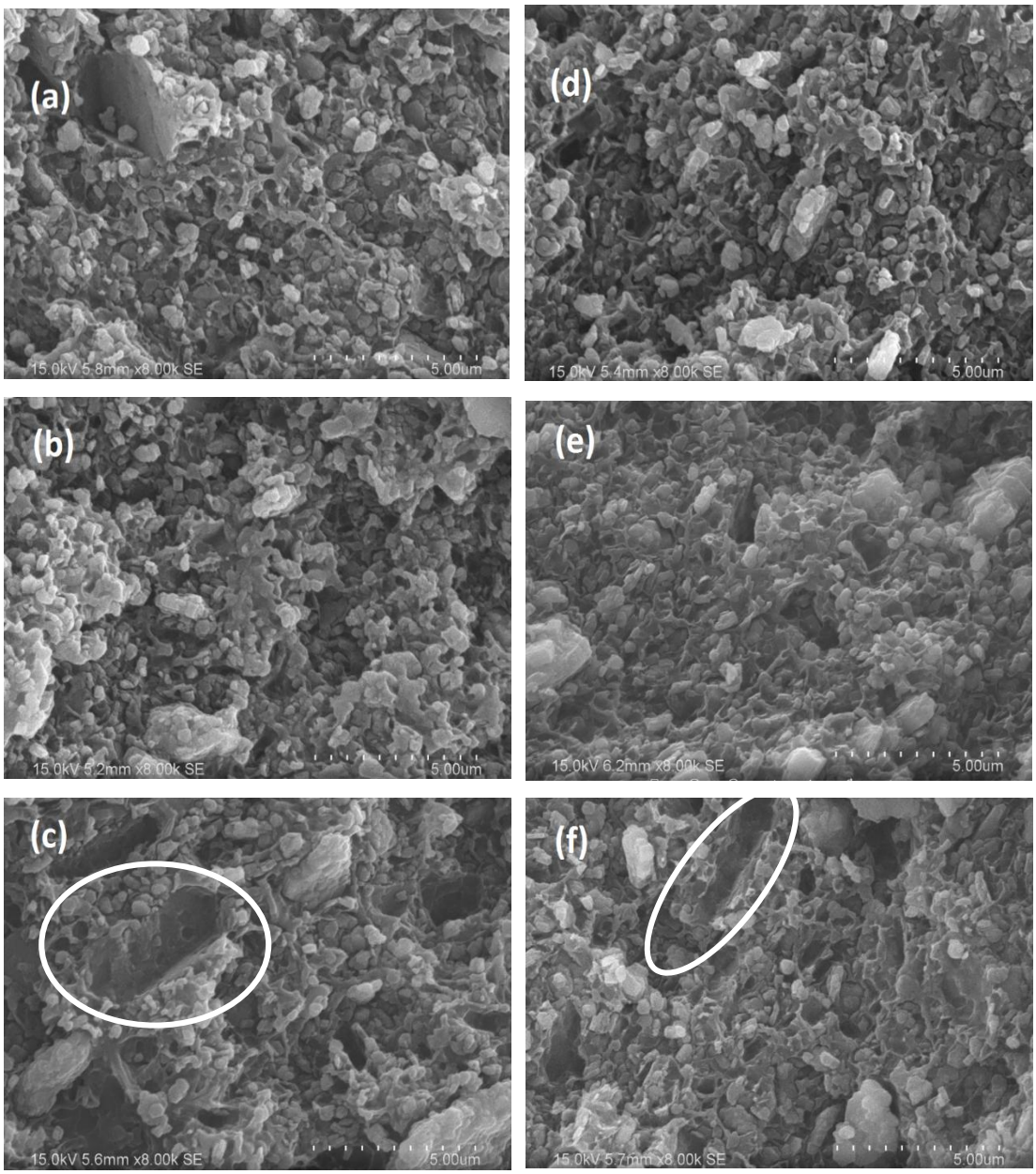

Figure 4.7: SEM Images of Fractured Surface of ATH added ABS composites for 100 phr (a) 50 kGy (b) 150 kGy (c) 250 kGy and for 120 phr (d) 50 kGy (e) 150 kGy and (f) 250 kGy.

As shown in Figure 4-8 the morphology of ATH added ABS composites has minimal differences. This could attribute to the small difference of tensile strength of different irradiation dosages. The amount of agglomeration as observed in the SEM images supports the high gel content and the low tensile strength for 140 phr of ATH added ABS composites.

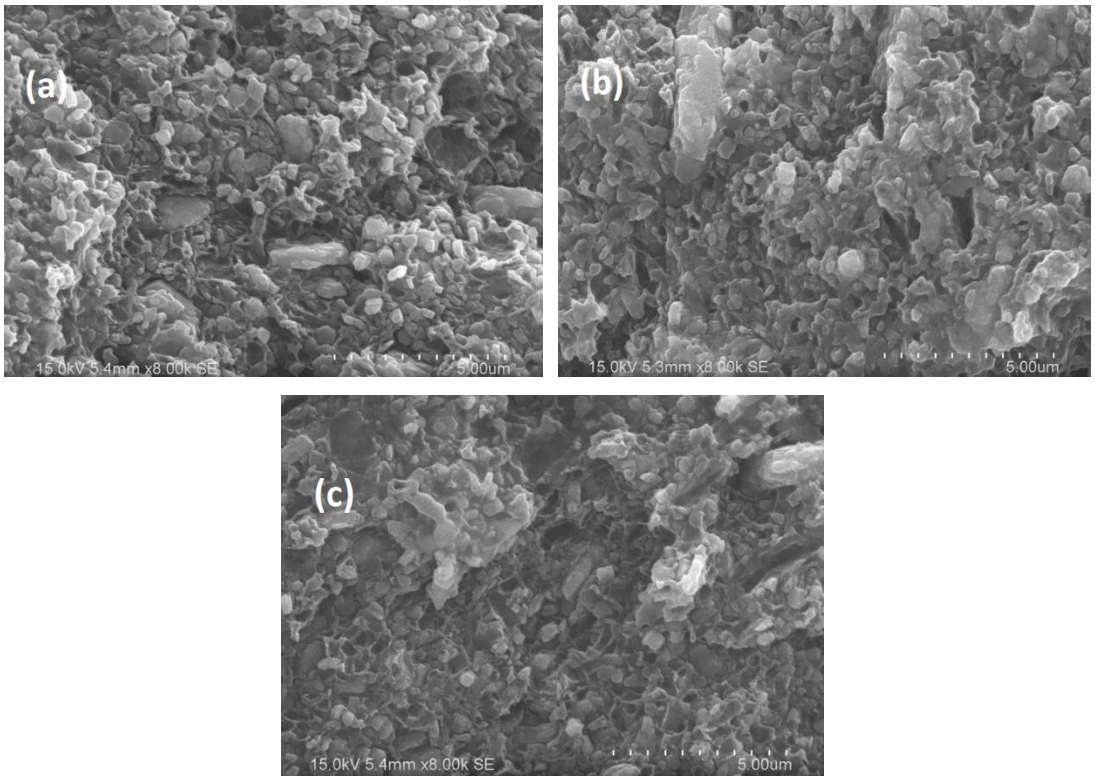

Figure 4.8: SEM images of Fractured Surface of ATH added ABS composites at 140 phr ATH with (a) 50 kGy, (b) 150 kGy, (c) 250 kGy

4.4 Limiting Oxygen Index

Limiting oxygen index test was conducted to determine the effect of ATH loading level and irradiation on the flame retardancy of ATH added ABS composites. The LOI value is a representation of the minimum required oxygen concentration in the mixture of nitrogen and oxygen to fuel the combustion process of a material. According to Figure 4.9, the limiting oxygen index (LOI) increased with increasing loading level of ATH for non-irradiated and irradiated ATH added ABS composites. The common LOI for pure ABS is 19 % where in this study the non-irradiated samples at 60 phr was able to produce 38.50 % of LOI. This shows that the ATH particles significantly enhanced the flame retardancy of ABS. The LOI value of 38.50 % indicated that the ATH added ABS composites required 38.50 % of oxygen to be ignited by a flame source. The high LOI proved the effective flame retardancy of ATH in ABS. Thermal degradation of ABS would reduce the molecular mass of

the ABS backbone chain and generated combustible polymer volatiles that could fuel the propagation of the combustion process. ATH had undergone endothermic reaction to produce alumina (char) and hydroxyl group that combined with the oxygen found in atmosphere and formed water vapour (Bonsignore, 1981). The water vapour diluted the combustible polymer volatiles surrounding the polymer and also reduced the temperature which would suppress the formation and spreading of flame. The formation of alumina (char) behaved like a thermal insulation layer on the polymer surface isolating the volatile polymers and oxygen gas. The insulation layer prevented heat exchange from the volatile polymers to the inner region of the polymer that would vaporize the combustible polymer volatiles to fuel the combustion process. Therefore it could further retard the combustion of the ABS matrix.

As shown in Figure 4.9 for all loading level of ATH, the LOI increased gradually with increasing irradiation dosage. This shows that the formation of crosslinking network in the ABS matrix could improve the flame resistance of ATH added ABS composites. The crosslinking network could increase the intermolecular forces within the ABS matrix and increased the thermal stability to resist the formation of volatile gases during combustion (Gad, 2009) and subsequently delayed the formation of flame. As shown in Figure 4.9, the effect of incorporating ATH into ABS on improving the LOI of ATH added ABS composites was the most significant from 80 phr to 100 phr. The LOI increased at an average of 16.6 % from 80 phr to 100 phr where the increment of LOI averaged at only 5.53 % from 60 phr to 80 phr. This shows that as the loading level of ATH achieved 100 phr the effect of ATH improved greatly. It is also observed that the increment of LOI from 100 phr to 140 phr was averaged at 9.69 % which shows that despite the gradual increasing loading level of ATH, the LOI increment is relatively small.

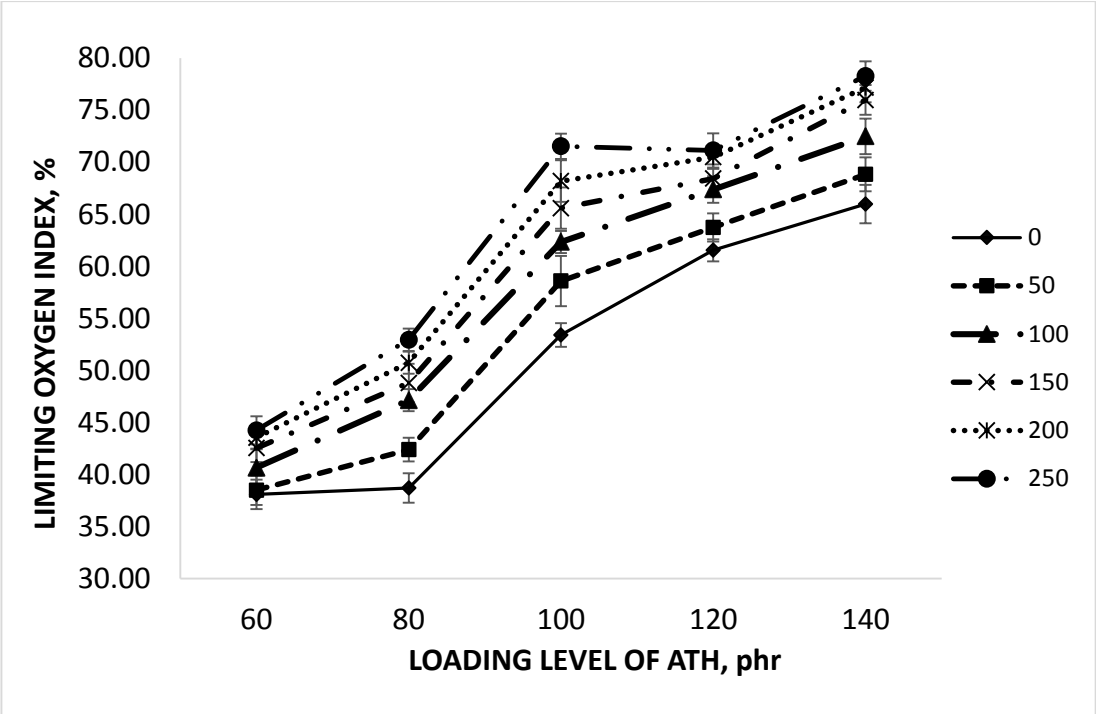

Figure 4.9: Effect of loading level of ATH on the limiting oxygen index

CHAPTER 5

CONCLUSION AND RECOMMENDATION

5.1 Conclusion

This study investigated the effects of ATH on the mechanical characteristics and flame retardancy of electron beam irradiated ABS samples. Increasing addition of ATH particles in non-irradiated samples ATH loading level had deteriorated the mechanical properties where the tensile strength reduced significantly because the poor interfacial adhesion of ATH and ABS matrix. ATH particles would cause the ABS matrix to agglomerate into larger particles and leading to low crystallinity in the ABS matrix. Low crystallinity was caused by irregular alignment in the polymer chains therefore it would deform easier when subjected to stretching. When the samples were subjected low irradiation dosage (50-100 kGy), the tensile strength of the samples improved due to the formation of crosslinking network as demonstrated by the increment in gel content value. The crosslinking network enhanced inter-chain interaction which would require more energy to break the forces. Among all the samples, the sample with 60 phr ATH exhibited the highest tensile strength. As further irradiation dosage was applied (150-250 kGy), the tensile strength of the samples deteriorated further due to the predominating chain scission reducing the density of crosslink network. Chain scission would reduce the molecular weight of the polymer chain and causing poor transfer of stress when stretched thus reducing the tensile strength of the polymer. The elongation at break was observed to be very low. The elongation at break was approximate ranged at 10 % to 14 %. The extendibility of the ATH added ABS was extremely small and exhibited low ductility. The young modulus for all samples except for 60 phr ATH, exhibited low value. This

shows the samples could elastically deform in a very small variation after the addition of 80-140 phr ATH. At 60 phr the young modulus exhibited high value showed that the crosslinking have strengthened the inter-chain bonding and resistance to stretching. The SEM images showed that ATH particles would form agglomerate in the ABS matrix and caused the formation of voids that contributed to the deterioration of mechanical properties. The discontinuous of ABS matrix as observed by SEM adhered to the reduction of the mechanical properties in the samples.

The LOI of all non-irradiated samples increased with increasing loading level of ATH from 60 phr to 140 phr. The increment in ATH particles would increase the formation of char and water vapour. The char formed would act as an insulation layer preventing the heat transfer from the volatiles polymers to the inner part of the polymer which would inhibit the combustion process. The formation of water vapour further retard the combustion process by diluting the combustible gas mixture and reduce the surrounding temperature. For all samples, the LOI increased with increasing irradiation dosage from 0 to 250 kGy. The increment in LOI could be attributed by the formation of crosslink network and increased the intermolecular forces that would require higher amount of energy to dissociate the molecular bonding. The steepest increased in LOI value could be observed at 100 phr which shows significant improvement in flame retardancy.

From the above observations, it can be concluded that the optimum amount of ATH required to achieve the required flame retardancy while maintaining mechanical, physical and thermal properties of ABS is 60 phr and the irradiation dosage that could improve the mechanical properties while maintaining an acceptable flame retardancy is 100 kGy.

5.2 Recommendation

It is recommended that the Thermogravimetric Analysis (TGA) analysis should be carried out in order to identify the mechanism of thermal decomposition of

composites during pyrolysis process. The mechanical properties of the samples deteriorated with increasing ATH particles therefore Transmittance Electron Microscopy (TEM) should also be conducted in this study in order to verify the agglomeration of ATH particles in the composites. The x-ray powder diffraction (XRD) is also recommended to be conducted in this study to determine the degree of crystallinity in the polymers.

REFERENCES

Abdul Aziz, A.A., Alauddin, S.M., Salleh, R.M. and Sabet, M., 2012. Influence of magnesium hydroxide/aluminum tri-hydroxide particle size on polymer flame retardancy: an overview. *International Journal of Chemical Engineering and Applications*, 3(6), pp. 437-440.

Akinay, A.E. and Tincer, T., 1999. Gamma-irradiated poly(tetrafluoroethylene) particle-filled low-density polyethylene. I. effect of silane coupling agents on mechanical, thermal, and morphological properties. *Journal of Applied Polymer Science*, 74(4), pp. 866-876.

ASTM Standard, 2001. D2765 *Standard Test Methods for Determination of Gel Content and Swell Ratio of Crosslinked Ethylene Plastics.* Annual Book of ASTM Standards.

ASTM Standard, 2008. D1822 *Standard Test Method for Tensile-Impact Energy to Break Plastics and Electrical Insulating Materials.* Annual Book of ASTM Standards.

ASTM Standard, 2008. D2863 *Standard Test Method for Measuring the Minimum Oxygen Concentration to Support Candle-Like Combustion of Plastics.* Annual Book of ASTM Standards.

ASTM Standard, 2010. D5510 *Standard Practice for Heat Aging of Oxidatively Degradable Plastics.* Annual Book of ASTM Standards

Baillet, C. and Delfosse, L., 1990. The combustion of polyolefins filled with metallic hydroxides and antimony trioxide. *Polymer Degradation and Stability,* 30, pp. 89–99.

Bee, S.T., Hassan, A., Ratnam, C.T., Tee, T.T., Lee, T.S. and Hui, D., 2014. Dispersion and roles of montmorillonite on structural, flammability, thermal and mechanical behaviours of electron beam irradiated flame retarded nanocomposites. *Composites Part B,* 61, pp. 41-48.

Bohen, J.M. and Lovenguth, R.F., 1989. *Tetrahalophthalate esters as flame retardants for certain resins.* WIPO Patent 1989003854.

Bonsignore, P.V. 1981. Alumina trihydarate as a flame retardant for polyurethane foams. In: K.C. Frisch and D. Klempner, eds. *Advances in urethane science and technology*. Pennsylvania: Technomic Publishing Co. Inc. pp. 253-262.

Bourbigot, S. and Duquesne, S., 2007. Fire retardant polymers: recent developments and opportunites. *Journal of Material Chemistry,* 17, pp. 2283-2300.

Browns, J.F., Clark, D. and Elliott, W.W., 1953. The thermal decomposition of the alumina trihydrate, gibbsite. *Journal of the Chemical Society,* pp. 84-88.

Brydson, J.A., 1999. *Plastics Materials.* 7th ed. Jordan Hill, Oxford: Butterworth-Heinemann.

Burger, W., Lunkwitz, K., Pompe, G., Petr, A. and Jehnichen, D., 1993. Radiation degradation of fluoropolymers-carboxylated fluoropolymers from radation degradation in presence of air. *Journal of Applied Polymer Science*, 48 (11) pp. 1973-1985.

Camino, G., Maffezzoli, A., Braglia, M., De Lazzaro, M. and Zammarano, M., 2001. Effects of hydroxides and hydroxycarbonate structure on fire retardant effectiveness and mechanical properties in ethylene-vinyl acetate copolymer. *Polymer Degradation and Stability,* 74, pp. 457-464.

Charlesby, A., 1977. Use of high energy radiation for crosslinking and degradation. *Radiation Physics and Chemistry*, 9, pp. 17-29.

Cheng, K.C., Yu, C.B., Guo, W., Wang, S.F., Chuang, T.H. and Lin, Y.H., 2012. Thermal properties and flammability of polyactide nanocomposites with aluminium trihydrate and organoclay. *Carbohydrate Polymers*, 87, pp. 1119-1123.

Ciullo, P.A., 1996. *Industrial minerals and their uses*. New Jersey, US: Noyes Publication.

Cleland, M.R., Parks, L.A. and Cheng, S., 2003. Application for radiation processing of materials. *Nuclear Instruments and Methods in Physics Research B,* 208, pp. 66-73.

Colborn, R.E., Buckley, D.J. and Adams, M.E., 1993. *Acrylonitrile-butdiene-styrene.* Shropshire, UK: iSmithers Rapra Publishing.

Cui, W., Guo, F. and Chen, J., 2007. Preparation and properties of flame retardant high impact polystyrene. *Fire Safety Journal,* 42, pp. 232-239.

Czvikovszky, T., 1996. Electron-beam processing of wood fiber reinforced polypropylene. *Radiation Physics and Chemistry,* 47(3), pp. 425-430.

De Chirico, A., Armanini, M., Chini, P., Cioccolo, G., Provasoli, F. and Audisio, G., 2003. Flame retardants for polypropylene based on lignin. *Polymer Degradation and Stability,* 79, pp. 139-145.

Delfosse, L., Baillet, C., Brault, A. and Brault, D., 1988. Combustion of ethylene-vinyl acetate copolymer filled with aluminium and magnesium hydroxides. *Polymer Degradation and Stability,* 23, pp. 337-347.

Derbyshire, R.L., 1980. *Treatment of sintered poly-tetrafluoro-ethylene with irradiation and heat to produce a grindable material*. US Patent 4748005.

Dunnick, J.K. and Nyska, A., 2009. Characterization of liver toxicity in F344/N rats and B6C3F1 mice after exposure to a flame retardant containing lower molecular weight polybrominated diphenyl ethers. *Experimental and Toxicologic Pathology,* 61(1), pp. 1-12.

Ebewele, R.O., 2000. *Polymer science and technology.* United States of America: Chapman & Hall/CRC Press LLC.

Gad, Y.H., 2009. Improving the properties of poly(ethylene-co-vinyl acetate)/clay composite by using electron beam irradiation. *Nuclear Instruments and Methods Physics Research Section B,* 267, pp. 3528-3534.

Giles, H.F. Jr., Wagner, J.R.Jr. and Mount, E.M.III., 2005. *Extrusion-the definitive processing guide and handbook.* United States of America; William Andrew Inc.

Guan, R., 2000. Structure and morphology of isotactic polypropylene functionalized by electron beam irradiation. *Journal of Applied Polymer Science,* 76(1), pp. 75-82.

Hornsby, P.R. and Watson, C.L., 1989. Mechanic aspects of smoke suppression and fire retardancy in polymers containing magnesium hydroxide filler. *Plastics and Rubber Processing and Applications,* 11, pp. 45-51.

Hornsby, P.R., 2001. Fire retardant fillers for polymers. *International Materials Reviews*, 46(4), pp. 199-210

Horrocks, A.R. and Price, D., 2001. *Fire retardant materials.* North America: CRC Press LLC.

Hull, T.R., Witkowski, A. and Hollingbery, L., 2011. Fire retardant action of mineral fillers. *Polymer Degradation and Stability,* 96, pp. 1462-1469.

Jia, X.W., 2005. Nano flame retardant material. *Industry Press*, pp. 250-273.

Kroschwitz, J.I., 1998. *Encyclopedia of Polymer Science and Engineering*, 2nd ed. New York: John Wiley & Sons,

Kulshreshtha, A.K. and Vasile, C., 2002. *Handbook of Polymer Blends and Composites, Volumes 1-4.* Shropshire, United Kingdom: Smithers Rapra Technology.

Laoutid, F., Bonnaud, L., Alexandre, M., Lopez-Custa, J.M. and Dubois, Ph., 2008. New prospect in flame retardant polymer materials: from fundatmental to nanocomposites. *Material Science and Engineering R,* 63, pp. 100-125.

Le Bras, M., Bourbigot, S., Duquesne, S., Jama, C. and Wilkie, C. eds., 2005. *Fire retardancy of polymers : new applications of mineral fillers*. Cambridge: The Royal Society of Chemistry.

Lee, S.Y., Song, JM., Sohn, JY., Shul, YG. And Shin, J., 2013. Radiation-induced crosslinking of poly(styrene-butadiene-styrene) block copolymers and their sulfonation. *Nuclear Instruments and Methods in Physics Research B,* 316, pp. 71-75.

Liu, M., Yin, Y., Fan, Z., Zheng, X., Shen, S., Deng, P., Zheng, C., Teng, H. and Zhang, W., 2012. The effects of gamma-irradiation on the structure, thermal resistance and mechanical properties of the PLA/EVOH blends. *Nuclear Instruments and Methods in Physics Research Section B*, 274, pp. 139-144.

Makuuchi, K. and Cheng, S., 2012. *Radiation processing of polymer materials and its industrial applications.* New Jersey: John Wiley & Sons.

Mapkar, J.A., 2008. Effect of elastomer functionalized carbon nano fiber-sheets. United States: Proquest LLC.

Mark, H.F., 2007. *Encyclopedia of Polymer Science and Technology, Concise.* United States: Wiley-Interscience.

Miller, A.A., 1959. Effects of high-energy radiation on polymers. *Annals of the New York Academy of Sciences,* 82, pp. 774-781.

Mouritz, A.P. and Gibson, A.G., 2007. *Fire Properties of Polymer Composite Materials.* Dordrecht, The Netherlands: Springer.

Murray, K.A., Kennedy, J.E., McEvoy, Brian., Vrain, O., Ryan, D., Cowman, R. and Higginbotham, C.L., 2013. Effect of gamma ray and electron beam irradiation on mechanical, thermal, structural and physicochemical properties of poly (ether-block-amide) thermoplastic elastomers. *Journal of The Mechanical Behaviour of Biomedical Materials,* 17, pp. 252-268.

Narkis, M., Sibony-Chaouat, S., Siegmann, A., Shkolnik, S. and Bell, J.P., 1985. Irradiation effects on polycaprolactone. *Polymer,* 26, pp. 50-54.

Ng, H.M., Bee, S.T., Ratnam, C.T., Lee, T.S., Phang, Y.Y., Tee, T.T. and Rahmat, A.R., 2014. Effectiveness of trimethylopropane trimethacrylate for the electron-beam-irradiation-induced cross-linking of polyactic acid. *Nuclear Instruments and Methods in Physics Research Section B,* 319, pp. 62-70.

Pal, G. and Macskasy, H., 1991. *Plastics: their behaviour in fires (studies in polymer science).* Translated from Hungarian Language by A.Grobler. New York: Elsevier Science Ltd.

Parkinson, W.W. and Sisman, O., 1971. The use of plastics and elastomers in nuclear radiation. *Nuclear Engineering and Design,* 17(2), pp. 247-280.

Rahman, F., Langford, K.H., Scrimshaw, M.D. and Lester, J.N., 2001. Polybrominated diphenyl ether PBDE flame retardants. *The Science of the Total Environment,* 275, pp. 1-17.

Ramani, R. and Ranganathaiah, C., 2000. Degradation of acrylonitrile-butadiene-styrene and polycarbonate by UV radiation. *Polymer Degradation and Stability,* 69, pp. 347-354.

Sun, Y., Matsumoto, M., Kitashima, K., Haruki, M., Kihara, S. and Takishima, S., 2014. Solubility and diffusion coefficient of supercritical-CO2 in polycarbonate and CO2 induced crystallization of polycarbonate. *The Journal of Supercritical Fluids*, 95, pp. 35-43.

Suzuki, M. and Wilkie, C.A., 1994. The thermal degradation of acrylonitrile-butadiene-styrene terpolymer as studied by TGA/FTIR. *Polymer Degradation and Stability,* 47, pp. 217-221.

Taniguchi, S., Sakuma, Yuichiro. and Yoshii, T., 1984. *Flame retardant additives based on alumina trihydrate and ethylene polymer compositions, containing same, having improved flame retardant properties.* US Patent 4430470.

Tiganis, B.E., Burn, L.S., Davis, P. and Hill, A.J., 2002. Thermal degradation of acrylonitrile-butadiene-styrene (ABS) blends. *Polymer Degradation and Stability,* 76, pp. 425-434.

Tillet, G., Boutevin, B. and Ameduri, B., 2011. Chemical reaction of polymer crosslinking and post-crosslinking at room and medium temperature. *Progress in Polymer Science,* 36(2), pp. 191-217.

Torikai, A., Murata, T. and Fueki, K., 1984. Radiation-induced degradation of polycarbonate: Electron spin resonance and molecular weight measurements. *Polymer Degradation and Stability,* 7(1), pp. 55-64.

United States Fire Administration, 2013. *Learn about fire: the nature of fire.* [Online] Available at < http://www.usfa.fema.gov/citizens/about_fire.shtm> [Accessed 3 August 2014]

Whelan, A., 1994. *Polymer Technology Dictionary.* London, UK: Chapman & Hall.

Wilkie, C.A. and Morgan, A.B. eds., 2010. *Fire retardancy of polymeric material.* United States of America: Taylor and Francis Group.

Wyzgoski, M.G., 1976. Effects of oven aging on ABS, poly(acrylonitrile-butadiene-styrene). *Polymer Engineering and Science,* 16(4), pp. 265-269.

Zaikov, G.E. and Lomakin, S.M., 2002. Ecological issue of polymer flame retardancy. *Journal of Applied Polymer and Science,* 86(10), pp. 2449-2462.

Zhang, X., Guo, F., Chen, J., Wang, G. and Liu, H., 2005. Investigation of interfacial modification for flame retardant ethylene-vinyl acetate copolymer/alumina trihydrate nanocomposites. *Polymer Degradation and Stability,* 87, pp. 411-418.